KINETIC STUDIES OF MIDDLE DISTILLATE FORMATION DURING CATALYTIC CRACKING OF HEAVY GAS OIL USING ZEOLITE-Y PREPARED FROMKANKARA-KAOLIN

BY

ADAM KEHINDE SALIHU

DEPARTMENT OF CHEMICAL ENGINEERING

AHMADU BELLO UNIVERSITY, ZARIA

NIGERIA.

FEBRUARY, 2015

KINETIC STUDIES OF MIDDLE DISTILLATE FORMATION DURING CATALYTIC CRACKING OF HEAVY GAS OIL USING ZEOLITE-Y PREPARED FROM KANKARA-KAOLIN

BY

Adam Kehinde SALIHU B.ENG (A.B.U. ZARIA) 2010
MSc/ENG/7553/2011-2012

A THESIS SUBMITTED TO THE SCHOOL OF POSTGRADUATE STUDIES, AHMADU BELLO UNIVERSITY, ZARIA

IN PARTIAL FULFILLMENT OF THE REQUIREMENTS FOR THE AWARD OF MASTER DEGREE IN CHEMICAL ENGINEERING.

DEPARTMENT OF CHEMICAL ENGINEERING,
FACULTY OF ENGINEERING
AHMADU BELLO UNIVERSITY, ZARIA
NIGERIA.

FEBRUARY, 2015

Declaration

I Adam Kehinde SALIHU, hereby declare that this thesis entitled **"CATALYTIC CRACKING OF HEAVY GAS OIL USING ZEOLITE Y PREPARED FROM KAOLIN: YIELD OF MIDDLE DISTILLATES"** has been carried out by me in the Department of Chemical Engineering and to the best of my knowledge has not been presented anywhere for the award of any degree. However, the information obtained from the literature has been duly acknowledged in the text and a list of references provided.

Adam Kehinde SALIHU ____________________ ____________________

Name of Student Signature Date

Certification

This is to certify that this thesis entitled **"CATALYTIC CRACKING OF HEAVY GAS OIL USING ZEOLITE Y PREPARED FROM KAOLIN: YIELD OF MIDDLE DISTILLATES"** by Adam, Kehinde SALIHU with registration number MSc/ENG/7553/2011-2012 meets the regulations governing the award of Master of Science (M.Sc) in Chemical Engineering of the Ahmadu Bello University, Zaria, and is approved for its contribution to knowledge and literary presentation.

Prof. A.S. Ahmed
Chairman, Supervisory Committee

Date

Dr O.A. Ajayi
Supervisory Committee

DateMember

Dr. B. Mukhtar
Member Supervisory Committee

Date

Dr. S. M. Waziri
Head of Department

Date

Prof. A.Z. Hassan
Dean, School of Postgraduate Studies

Date

Acknowledgements

My deepest and greatest gratitude goes to Almighty Allah for His love and kindness in making this thesis a huge success. May His peace be upon the last prophet, Muhammad (S.A.W), his entire family and those that follow his footsteps until the Last Day.

My profound appreciation goes to my lovely parent, Mr. and Mrs. Salihu, brothers and sisters for their sacrifice and prayer in the course of my academic pursuit.

My sincere appreciation goes to my major supervisor Prof. A.S. Ahmed and his colleagues in the supervisory team; Dr. O.A. Ajayi and Dr. B. Mukhtar, for their valuable times and motivations given to me during the entire life span of this thesis. I wish to express my immense gratitude to Dr. B.O. Aderemi for his encouragement, input and suggestions, may God’s blessings be with him and his family.

I wouldn’t forget the contribution of the PTDF research team: Suleiman Yunusa, Nurudeen Salaudeen, Solomon Gajere Bawa, Mustapha Yusuf and Sani Nakakana towards making the work worthwhile.

I wish to lodge my vote of thanks to all the lecturers of Chemical Engineering Department, Ahmadu Bello University who have left no stone unturned to ensure I acquired all requisite knowledge to face the future challenges.

My final appreciation goes to all those special individuals, colleagues, family members and friends who I cannot all mention here and have contributed in one way or the other towards me being what I am today. I am indeed very grateful.

Dedication

This project work is dedicated to the entire family of Mr. Salihu Abdulqadir for their immeasurable contribution towards me being what I am today.

ABSTRACT

In the economy of a modern refinery, fluid catalytic cracking unit (FCCU) plays a significant role, as it adds value to the refinery products. In this unit more attention is usually given to the behavior of gasoline formation, but it is also important to study the manner of the middle distillates (kerosene and diesel) formation during the cracking process. In the present study, catalytic crackingof heavy gas oil on FCC type catalysts (zeolite Y, blend of zeolite Y (75%) and ZSM-5 zeolite (25%) and commercial zeolite Y)was carried out in a bench scale mini-fluidized bed reactor.The activities of the two prepared catalysts from kaolin were compared with commercial zeolite Y used by Kaduna Refinery and Petrochemical Company (KRPC).The feed in this study was heavy gas oil (also obtained from KRPC); the cracking process was carried out at reaction temperature of 500-590˚C and reaction time of 30-180 seconds. The yields of kerosene and diesel fractions were observed to decrease with time at 500˚C and 530˚C but increased with time at 560˚C and 590˚C for all the catalysts. In terms of catalytic activity amongst the three catalysts, analysis of the products shows that the zeolite blend (i.e. zeolite Y/ZSM-5) was most active with superior product selectivity for the lighter fractions. With the zeolite blend, the yields of kerosene and diesel were found to be lowest at 17.63% and 15.56% respectively.This indicatedthe effect of ZSM-5 in converting the heavier fractions in the middle distillate range to lighter fractions. Synthesized zeolite Y had 19.8% and 21.27% yield of kerosene and diesel fractions respectively while the commercial zeolite Y gave 32.29% and 19.04% yields of kerosene and diesel fractions respectively.

TABLE OF CONTENTS

LIST OF FIGURES

LIST OF TABLES

LIST OF ABBREVIATIONS

HGO	Heavy gas oil
API	American Petroleum Institute
LPG	Liquid Petroleum Gas
FCCU	Fluidized Catalytic Cracking Unit
LCO	Light Cycle Oil
UCS	Unit cell size
SAR	Silicon to aluminum ratio
SBU	Secondary building unit
FAU	Faujasite
Scfh	Standard cubic feet per hour
C_p	Concentration of product component
W_{HGO}	Weight of Heavy Gas Oil
W_p	Weight of product component

LIST OF SYMBOLS

A_0	Arrhenius constant or pre-exponential factor
C_g	concentration of gases
C_{go}	concentration of gas oil
E_a	Activation energy
k	rate constant
k_{comY1}	rate constant for first order kinetics using commercial zeolite Y
k_{comY2}	rate constant for second order kinetics using commercial zeolite Y
k_{synY}	rate constant using synthesized zeolite Y
R	molar gas constant
R^2	Correlation coefficient
r_c	rate of reaction of coke
r_g	rate of reaction of gas
r_{go}	rate of reaction of gas oil
r_{lg}	rate of reaction of light gases
t	Contact time
T	Temperature
X_t	Conversion of HGO at a particular contact time
X_T	Conversion of HGO at a particular temperature
Φ	Catalyst activity coefficient

CHAPTER ONE

INTRODUCTION

1.1 PREAMBLE

Energy is vital for the development of human society.It is associated with several aspects of the social activities and daily life. With increasing world population and rising living standards, the demand for energy is steadily increasing in the world. As energy is an important resource, its cheap and stable supply is necessary to safeguard the economy and social development. Developing countries face the double pressure of economic growth and environmental protection as they enter the 21st century. Petroleum has become more and more important to the world's economy, so important that today, without a steady flow of oil, most human activities on this planet would grind to a halt (Ahmed *et al*., 2007). Petroleum provides fuels and lubricants for vehicles and precursors for the world's petrochemical industries. The fuels that are derived from petroleum supply more than half of the world's total supply of energy (Ahmed *et al*., 2007). Refining of crude oil results in more valuable products such as gasoline, kerosene, and diesel oil.

The world production of petroleum has been stagnant for the past few years because of the lack of discovery of new sites. Even though, there are reports that few new sites have been found to contain petroleum, the world production of petroleum is insufficient to meet the demand. In many parts of the world, liquid fuel production is declining and heavy oil conversion, therefore, becomes important to maintain economic viability of these regions.

The majority of machinery and equipment manufactured at present are designed to run using liquid fuel (gasoline, kerosene and diesel). For this reason, it is important to extract much useful products from crude oil. The ongoing trends in the petroleum refining industry have resulted in the need to upgrade heavy oils that otherwise are difficult to transport and market due to their high viscosity and high levels of contaminants such as sulphur, metals, asphaltenes, carbon residues and solid particles. These have made the conversion of heavy petroleum fraction into valuable liquid products to be one of the most important objectives for upgrading heavy petroleum oils.

The conversion of heavy petroleum fraction into valuable products has been achieved mainly by thermal cracking, catalytic cracking and hydrocracking (Ahmed *et al*., 2007). In thermal cracking process, hydrocarbons with higher molecular weight in heavy oils are transformed to lighter hydrocarbon products by thermolysis at a higher temperature, which is accompanied with the formation of coke. The development of thermal cracking process for producing middle distillates has been limited because large amounts of gas and naphtha with lower quality are produced due to over cracking (Ronald *et al*., 1999).

Catalytic cracking is different from thermal cracking because carbon-carbon bond cleavage of hydrocarbons in the former occurs on a solid acid catalyst. However, the absence of a high partial pressure of hydrogen in the catalytic cracking process not only makes possible the rapid build-up of coke on the catalyst but also results in products containing a significant amount of olefinic and aromatic compounds, the primary goal of this process is usually for the production of gasoline and the secondary products are kerosene and diesel but there is also need the to study the manner in which this process behaves towards the yield of the secondary products. Hydrocracking process uses a metal supported solid acid catalyst producing high quality motor fuels. Hydrocracking reactions proceed through a bi-functional mechanism. A bi-functional mechanism is one that requires two distinct types of catalytic sites to catalyze separate steps in the reaction sequence. These two functions are the acid function, which provide for the cracking and isomerization and the metal function, which provide for the olefin formation and hydrogenation.

Zeolites and related crystalline molecular sieves are widely used as cracking catalysts in the industry since they possess catalytically active sites as well as uniformly sized and shaped micro-pores that allow for their use as shaped selective catalysts in oil refining, petro-chemistry and organic synthesis. However, due to the pore size constraints, the unique catalytic properties of zeolites are limited to reactant molecules having kinetic diameters below 10 Å (Ronald *et al*., 1999). Zeolites have been successful because of their crystallinity, high surface area, adsorption capacity, and uniform size distribution which enable shape selectivity (Den-Hollander *et al*. 2002).

The main goal of this work was to test the performance and kinetic parameters of zeolite Y synthesized from kaolin in cracking of heavy gas oil towards the yield of the middle distillates. For this purpose, different operating conditions were varied to determine the optimum for the conversion of heavy gas oil.

1.2 Problem Statement

Detailed study on the performance of zeolite Y prepared fromKankara-kaolin has not been carried out on catalytic cracking of heavy gas oil to obtain middle distillates. The complexities of the heavy gas oil mixture have posed a challenge in obtaining experimental data during cracking of heavy gas oil.

1.3 Justification

- The outcome of this study will assist in the development of a high performance zeolite through modification of the method of synthesis fromKankara-kaolin.

- Certainparameters required for catalytic reactor design will be obtained and provide experimental data for kinetic modeling.

1.4 Aim and Objectives

The aim of this research work is to study the performance of zeolite Y prepared from Kankara kaolin on thecatalytic cracking of heavy gas oil (HGO) to kerosene and diesel fractions.

The specific objectives are:

- To test the activity of the zeolite in the catalytic cracking process.
- To investigate its performance towards kerosene and diesel fractions.
- To study the effects of temperature and time on the conversion of heavy gas oil and the yield of the middle distillates (kerosene and diesel).
- To study the kinetics of the catalytic reaction.
- To study the effect of blending ZSM-5 and zeolite Y in catalytic cracking of HGO.

1.5 Scope of Work

The scope of the research involve catalytic cracking of heavy gas oil using the zeolite Y prepared from local raw materials where the operating temperature was varied between 500˚C and 590˚C and the reaction time for the reaction was varied between 30 seconds and 180 seconds. During this reaction, time, conversion of the hydrocarbon and activity of the catalysts were monitored. The products obtained were analyzed using gas chromatography. This research work attempts to fill the bridge of the use of catalyst (zeolite Y) prepared from Kankara-kaolin for cracking of heavy gas oil compared to the FCCU catalyst and also to study the effect of blending zeolite ZSM-5 in the prepared catalyst.

CHAPTER TWO
LITERATURE SURVEY

2.1 Petroleum

Petroleum (also called crude oil) is perhaps one of the most important substances consumed in modern society. It provides not only raw materials for the plastics and other products but also fuel for energy, industry, heating, and transportation. The oil industry classified crude oil by its origin, for example, West Texas Intermediate, Brent and often by its relative weight or viscosity: light, intermediate or heavy (Abdel-Aal, *et al*., 2003). Refiners may also refer to it as "sweet," which means it contains relatively little sulphur, or as "sour," which means it contains substantial amounts of sulphur and requires more refining in order to meet current product specifications.

The word petroleum, derived from the Latin petra and oleum, means literally “rock oil” and refers to hydrocarbons that occur widely in the sedimentary rocks in the form of gases, liquids, semisolids, or solids (Speight, 2007). Petroleum is generally considered to be formed from animal and vegetables debris accumulating in sea basins or estuaries and buried there by sand and salt. The debris may have been decomposed by anaerobic bacteria under reducing conditions, so that most of the oxygen is removed, or oil may have been distilled from the partially decayed debris by heat generated by earth movements or by depth of burial (Erikh *et al*., 1988). The final result is a black viscous very complex mixture containing many different hydrocarbon compounds like paraffin, naphthene and aromatic hydrocarbons that vary in appearance and composition from one oil field to another. On average, crude oil contains about 84-87% carbon, 11-14% hydrogen, 0.06-8% sulphur, 0.02-1.7% nitrogen, 0.68-1.82% oxygen, 0.00-0.14% metals (Erikh *et al*., 1988).

Petroleum varies dramatically in colour, odour, and flow properties that reflect the diversity of its origin as shown in Table 2.1. The majority products of crude oil are liquified petroleum gas (LPG), gasoline, kerosene, diesel, gas oil and residues. Table 2.1 summarized product types and carbon number range. These products are separated by distillation in refinery.

Table 2.1: Compositions (residuum content) and properties (specific gravity and API gravity) of various crude oil from different locations.

Crude oil	Specific gravity	API gravity	Residuum > 1000˚F
California	0.858	33.4	23.0
Oklahoma	0.816	41.9	20.0
Pennsylvania	0.800	45.4	2.0
Texas	0.827	39.6	15.0
Bahrain	0.861	32.8	26.4
Iran	0.836	37.8	20.8
Iraq	0.844	36.2	23.8
Kuwait	0.86	33.0	31.9
Saudi Arabia	0.84	37.0	27.5
Venezuela	0.95	17.4	33.6

Adopted from Speight, 2007

Distillation is the separation of crude oil in atmospheric and vacuum distillation columns into groups of hydrocarbon compounds of different boiling point ranges called fractions or cuts (Speight, 2007). Figure 2.1 shows schematic diagram of crude oil refinery distillation column (Speight, 2006).

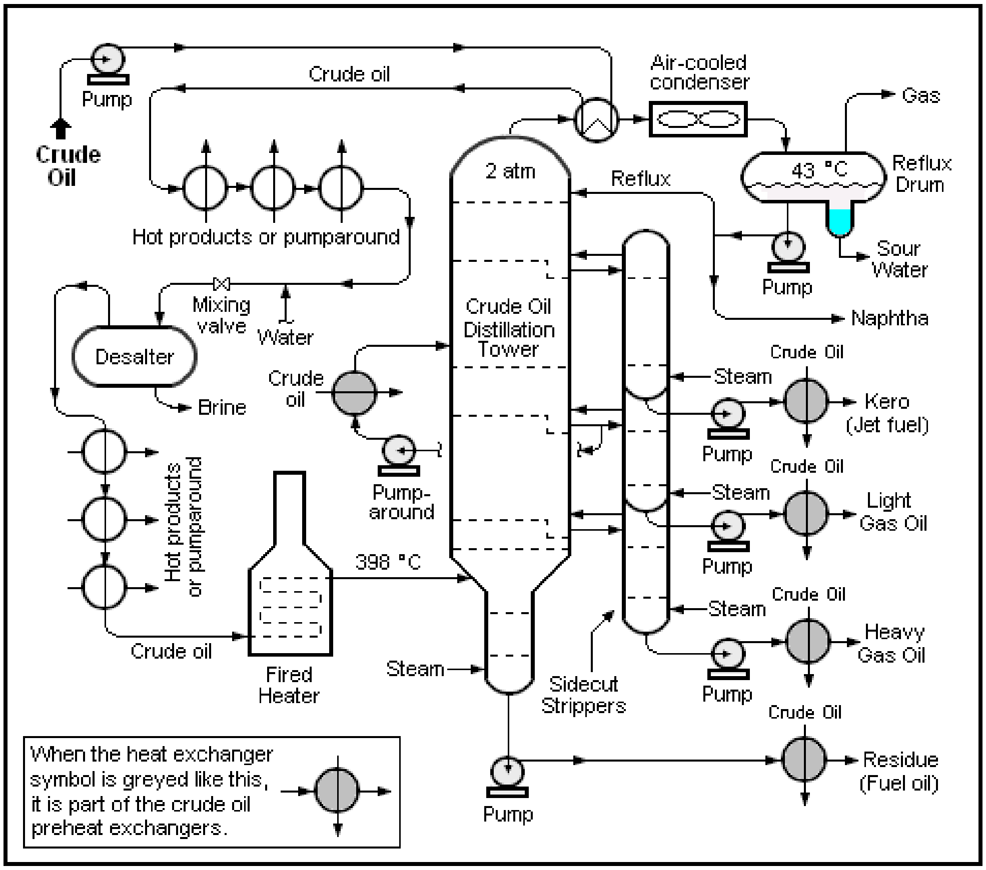

Figure 2.1: Schematic diagram of crude oil refinery distillation column

2.2 Gas Oil

Gas oil is the fraction of crude oil, which is obtained by atmospheric or vacuum distillation of crude oil, and the boiling range from petroleum is between 215˚C - 337˚C (light gas oil) or 320˚C - 426˚C (heavy gas oil) (Ahmed *et al*., 2007). Gas oil consists of a homogeneous mixture of hydrocarbon compounds which contain carbon and hydrogen, further heterogeneous hydrocarbon compounds which contain sulphur (for example hydrogen sulphide and methyl mercaptan), nitrogen (i.e andole and carbazole) and oxygen (i.e. methyl alcohol and acetic acid) as well as very small amounts of non-hydrocarbon metallic compounds such as iron, copper, nickel and vanadium (Speight, 2007). Representative properties of light and heavy gas oil are shown in Table 2.2 and their properties are shown in Table 2.3.

Table 2.2: General summary of product types and their carbon number range

Product	Lower carbon	Upper carbon
Refinery gas	C1	C4
Liquified petroleum gas	C3	C4
Naphta	C5	C17
Gasoline	C4	C12
Kerosene/diesel fuel	C8	C18
Aviation turbine fuel	C8	C16
Gas oil	C12	>C20
Lubricating oil	>C20	-
Wax	C17	>C20
Asphalt	>C20	-
Coke	>C50	-

Adopted from Speight, 2007

Gas oil is also classified based on production process from crude oil by various refining processes. There are six groups allocated to the refining process namely:

1. Straight-run gas oils obtained by the atmospheric distillation of crude oil (straight-run gas oil).
2. Cracked gas oils obtained from refinery feedstock by thermal, catalytic or steam cracking processes (cracked gas oil).
3. Hydrocracked gas oils obtained from refinery feedstock by simultaneous processes of cracking and hydrogenation (cracked gas oil).

4. Gas oil distillate fuels normally obtained by blending straight-run, cracked and hydrocracked gas oils (gas oil - unspecified).
5. Distillates obtained by vacuum distillation of the residues left after the atmospheric distillation of crude oil (vacuum gas oil).
6. Other gas oils obtained when straight-run or cracked gas oils are subjected to further refining processes (gas oil - unspecified).

Speight, (2007) reported that straight-run and vacuum gas oils typically contain 70-80% aliphatic hydrocarbons, 20-30% aromatic hydrocarbons and less than 5% of olefins whereas cracked gas oils may contain up to 75% of aromatic hydrocarbons and up to 10% olefins. Since part of the gas oils are distilled at temperatures in excess of 350°C, they may contain minor concentrations of 4 to 6 ring polycyclic aromatic hydrocarbons.

Table 2.3: Properties of light and heavy gas oil

Property	Light gas oil	Heavy gas oil
Flash point, ˚C, minimum	38	38
Pour point, ˚C, maximum	-18	-6
Initial boiling point, ˚C	215	320
Final boiling point, ˚C	337	426
Viscosity, mm^2/s, 40˚C, minimum	1.3	1.9
Viscosity, mm^2/s, 40˚C, maximum	2.1	3.4
Density, kg/m^3, 15˚C, (API)	850 (35)	876 (30)
Ramsbottom carbon residue, wt%	0.15	0.35
Sulphur, wt%	0.5	0.5
Water and sediment, vol%	0.05	0.05

Adopted from Ahmed *et al*., 2007

The ever increasing demand for lighter engine fuel and higher price of light crude oil have stimulated the petroleum refining industry into looking for the possibility of processing heavy fractions as well as the comparatively cheaper heavy crude oils. Therefore, to meet the growing demand for lighter fuel the need for more efficient process is necessary. One of these processes in the petroleum refinery is the catalytic cracking of heavy hydrocarbons using Fluidized Catalytic Cracking Unit (FCCU).

2.3 Hydrocarbon Cracking Processes

2.3.1 Thermal cracking process

The term cracking applies to the decomposition of petroleum constituents that is induced at elevated temperatures (>500˚C), whereby the higher molecular weight constituents of petroleum are converted (broken down) to lower molecular weight products. Cracking reactions involve carbon–carbon bond rupture and are thermodynamically favored at high temperature (Ronald *et al*., 1999).

Thus, cracking is a phenomenon by which higher boiling (higher molecular weight) constituents in petroleum are converted into lower boiling (lower molecular weight) products. However, certain products may interact with one another to yield products with higher molecular weights than the constituents of the original feedstock. Some of the products include gases, gasoline-range materials, kerosene-range materials, diesel range materials and the various intermediates that produce other products such as coke. Mixtures of products that have boiling ranges higher than gasoline and kerosene may (depending upon the refining options) be referred to as recycle stock, which is recycled in the cracking equipment until conversion is complete (Speight, 2007).

Two general types of reaction occur during cracking:

1. The decomposition of large molecules into small molecules (primary reactions), for example:

$$\underset{\text{Butane}}{CH_3CH_2CH_2CH_3} \longrightarrow \underset{\text{Methane}}{CH_4} + \underset{\text{Propene}}{CH_3CH{=}CH_2} \quad \ldots (1)$$

$$CH_3CH_2CH_2CH_3 \longrightarrow CH_3CH_3 + CH_2{=}CH_2 \quad \ldots (2)$$

2. Reactions by which some of the primary products interact to form higher molecular weight materials (secondary reactions):

$$CH_2{=}CH_2 + CH_2{=}CH_2 \longrightarrow CH_3CH_2CH{=}CH_2 \quad \ldots (3)$$

$$R_2CH{=}CH_2 + R_1CH{=}CH_2 \longrightarrow \text{Cracked residuum+Coke + Other products} \quad \ldots (4)$$

Thermal cracking is a free radical chain reaction; a free radical is an atom or group of atoms possessing an unpaired electron. Free radicals are very reactive, and it is their mode of reaction that actually determines the product distribution during thermal cracking. The free radical reacts with a hydrocarbon by abstracting a hydrogen atom to produce a stable end product and a new free radical. Free radical reactions are extremely complex and many of the reactions are feasible, but the product distributions in thermal cracking are usually determined by the reaction favored thermodynamically (Harold *et al*., 2004).

One of the significant features of hydrocarbon free radicals is their resistance to isomerization (Speight, 2007), for example, migration of an alkyl group and, as a result, thermal cracking does not produce any degree of branching in the products other than that already present in the feedstock.

Data obtained from the thermal decomposition of pure compounds indicate certain decomposition characteristics that permit predictions to be made of the product types that arise from the thermal cracking of various feedstocks. For example, normal paraffins are believed to form, initially, higher molecular weight material, which subsequently decomposes as the reaction progresses. Other paraffinic materials and olefins are produced.

An increase in pressure inhibits the formation of low-molecular weight gaseous products and therefore promotes the formation of higher molecular weight materials (Ronald *et al.*, 1999). Branched paraffins react somewhat differently to the normal paraffins during cracking processes and produce substantially higher yields of olefins with one less carbon atom than the parent hydrocarbon. Cyclo-paraffins (naphthenes) react differently to their noncyclic counterparts and are somewhat more stable. For example, cyclohexane produces hydrogen, ethylene, butadiene, and benzene: alkyl-substituted cyclo-paraffins decompose by means of scission of the alkyl chain to produce an olefin and a methyl or ethyl cyclohexane.

The aromatic ring is considered fairly stable at moderate cracking temperatures (350˚C to 500˚C). Alkylated aromatics, like the alkylated naphthenes, are more prone to dealkylation than to ring destruction. However, ring destruction of the benzene derivatives occurs above 500˚C, but condensed aromatics may undergo ring destruction at somewhat lower temperatures (450˚C) (Speight, 2007).

2.3.2 Mechanism of thermal cracking

Thermal cracking depends on temperature and time. Cracking of hydrocarbons here occurs in the absence of a catalyst, exposed to high temperatures in the range of 425°C to 650°C.

Thermal cracking is initiated by the formation of free radicals by the cleavage of C-C bond. The splitting produces two uncharged species (called free radicals) that share a pair of electrons.

Equation (5) shows the formation of free radicals when a hydrocarbon is thermally cracked:

$$R_1\text{-}CH_2\text{-}CH_2\text{-}R_2 \longrightarrow R_1\text{-}\cdot CH_2 + \cdot CH_2\text{-}R_2 \qquad \ldots (5)$$

These free radicals formed are very unstable, extremely reactive and short-lived; they can undergo alpha scission (one carbon away from the free radical), beta scission (two carbons away from the free radical), and polymerization.

Beta-scission is the most favorable form of scission of the hydrocarbons as alpha-scission is not thermodynamically favored but it occurs. Beta-scission produces an olefin (ethylene) and a primary free radical which has two fewer carbon atoms as shown in equation (6):

$$R\text{-}CH_2\text{-}CH_2\text{-}\cdot CH_2 \longrightarrow R\text{-}\cdot CH_2 + CH_2{=}CH_2 \qquad \ldots (6)$$

The primary free radical can further undergo beta-scission to yield more ethylene. Unlike beta-scission, alpha scission produces a methyl radical, which can extract a hydrogen atom from a neutral hydrocarbon molecule which yields methane and a secondary or tertiary free radical as shown in equation (7):

$$H_3{\cdot}C + R\text{-}CH_2\text{-}CH_2\text{-}CH_2\text{-}CH_2\text{-}CH_2\text{-}CH_2\text{-}CH_3 \longrightarrow$$

$$CH_4 + R\text{-}CH_2\text{-}CH_2\text{-}CH_2\text{-}CH_2\text{-}{\cdot}CH\text{-}CH_2\text{-}CH_3 \qquad \ldots (7)$$

This secondary radical formed can undergo beta-scission; the products will be an alpha-olefin and a primary free radical.

$$R\text{-}CH_2\text{-}CH_2\text{-}CH_2\text{-}CH_2\text{-}{\cdot}CH\text{-}CH_2\text{-}CH_3 \longrightarrow$$

$$R\text{-}CH_2\text{-}CH_2\text{-}{\cdot}CH_2 + H_2C{=}CH\text{-}CH_2\text{-}CH_3 \qquad \ldots (8)$$

Similar to the methyl radical, the $R\text{-}{\cdot}CH_2$ radical can also extract a hydrogen atom from another paraffin to form a secondary free radical and a smaller hydrocarbon, except that $R\text{-}{\cdot}CH_2$ is more stable than ${\cdot}CH_3$, hence the hydrogen extraction rate of $R\text{-}{\cdot}CH_2$ is lower than that of methyl radical (Bruce *et al*., 1979). Consequently, the sequence of reaction forms a product rich in C1 and C2 and a little amount of alpha olefins.

One of the drawbacks of thermal cracking in an FCCU is that a high percentage of the olefins formed during intermediate reactions polymerize and condense directly to coke(Bruce *et al*., 1979).

2.3.3 Catalytic cracking process

Catalytic cracking processes evolved in the 1930s, from research on petroleum and coal liquids. Catalytic cracking is the thermal decomposition of petroleum constituents hydrocarbons in the presence of a catalyst (Ronald *et al*., 1999). Thermal cracking has been superseded by catalytic cracking as the process for gasoline manufacture. Products from catalytic cracking process are richer in branched paraffins, cyclo-paraffins, and aromatics, all of which serve to increase the quality of the liquid products. Catalytic cracking also results in production of the maximum amount of butenes and butanes (C_4H_8 and C_4H_{10}), rather than ethylene and ethane (C_2H_4 and C_2H_6) (Harold *et al*., 2004).

Although thermal cracking is a free radical (neutral) process, catalytic cracking is an ionic process involving carbocations (carbenium or carbonium ions) which are hydrocarbon ions having a positive charge on a carbon atom. The formation of carbonium ions during catalytic cracking can occur by:

1. Addition of a proton from an acid catalyst to an olefin.

2. Abstraction of a hydride ion (H^-) from a hydrocarbon by the acid catalyst or by another carbonium ion.

However, carbonium ions are not formed by cleavage of a carbon–carbon bond. In essence, the use of a catalyst permits alternate routes for cracking reactions, usually by lowering the free energy of activation for the reaction. The acid catalysts first used in catalytic cracking were amorphous solids composed of approximately 87% silica (SiO_2) and 13% alumina (Al_2O_3) and were designated low-alumina catalysts (Bruce *et al*., 1979). However, these type of catalysts are now being replaced by crystalline aluminosilicates (zeolites) or molecular sieves.

The first catalysts used for catalytic cracking were acid - treated clays, formed into beads. In fact, clays are still employed as catalyst in some cracking processes. Clays are a family of crystalline aluminosilicate solids, and the acid treatment develops acidic sites by removing aluminum from the structure. The acid sites also catalyze the formation of coke, and the development of a moving - bed process that continuously removed the coked beads from the reactor reduced the yield of coke; clay regeneration was achieved by oxidation with air (Speight, 2007).

Clays are natural compounds of silica and alumina, containing major amounts of the oxides of sodium, potassium, magnesium, calcium, and other alkali and alkaline earth metals. Iron and other transition metals are often found in natural clays, substituted for the aluminum cations. Oxides of virtually every metal are found as impurity deposits in clay minerals. Clays are layered crystalline materials. They contain large amounts of water within and between the layers (Ronald *et al.*, 1999). Heating the clays above 100˚C can drive out some or all of this water; at higher temperatures, the clay structures themselves can undergo complex solid state reactions. Such behavior makes the chemistry of clays a fascinating field of study in its own right. Typical clays include kaolinite, montmorillonite, and illite (Harold *et al*., 2004). They are found in most natural soils and in large, relatively pure deposits, from which they are mined for applications ranging from adsorbents to paper making.

Once the carbonium ions are formed, the modes of interaction constitute an important means by which product formation occurs during catalytic cracking. For example, isomerization either by hydride ion shift or by methyl group shift, both of which occur readily. The trend is for stabilization of the carbonium ion by movement of the charged carbon atom toward the center of the molecule, which accounts for the isomerization of α-olefins to internal olefins when carbonium ions are produced. Cyclization can occur by internal addition of a carbonium ion to a double bond which, by continuation of the sequence, can result in aromatization of the cyclic carbonium ion.

Like the paraffins, naphthenes do not appear to isomerize before cracking. However, the naphthenic hydrocarbons (from C9 upward) produce considerable amounts of aromatic hydrocarbons during catalytic cracking. Alkylated benzenes undergo nearly quantitative dealkylation to benzene without apparent ring degradation below 500˚C. However, polymethlybenzenes undergo disproportionation and isomerization with very little benzene formation (Bruce *et al.*, 1979).

Catalytic cracking can be represented by simple reaction schemes. The Lewis site mechanism is the most obvious; as it proposes that a carbenium ion is formed by the abstraction of a hydride ion from a saturated hydrocarbon by a strong Lewis acid site (a tri coordinated aluminum species). On Brønsted sites, a carbenium ion may be readily formed from an olefin by the addition of a proton to the double bond.

The earliest cracking mechanisms postulated that the initial carbenium ions are formed only by the protonation of olefins generated either by thermal cracking or present in the feed as an impurity. For a number of reasons this proposal was not convincing, and in the continuing search for initiating reactions it was even proposed that electrical fields associated with the cations in the zeolite are responsible for the polarization of reactant paraffins, thereby activating them for cracking. More recently, however, it has been convincingly shown that a penta-coordinated carbonium ion can be formed on the alkane itself by protonation, if a sufficiently strong Brønsted proton is available (Hollander *et al.*, 2002).

Coke formation is considered, with just cause as a malignant side reaction of normal carbenium ions. However, while chain reactions dominate events occurring on the surface, and produce the majority of products, certain less desirable bimolecular events have a finite chance of involving the same carbenium ions in a bimolecular interaction with one another.

A general reaction sequence for coke formation from paraffins involves oligomerization, cyclization, and dehydrogenation of small molecules at active sites within zeolite pores:

Alkanes $\longrightarrow$ Alkenes

Alkenes $\longrightarrow$ Oligomers

Oligomers $\longrightarrow$ Naphthenes

Naphthenes $\longrightarrow$ Aromatics

Aromatics $\longrightarrow$ Coke

This is a summary of the basic steps to coke formation. The problem with this reaction sequence is that it ignores sequential reactions in favor of consecutive reactions. And it must be accepted that the chemistry leading up to coke formation is a complex process, consisting of many sequential and parallel reactions.

2.3.4 Mechanism of catalytic cracking

When the feed come in contact with the catalyst in the reactor which is at the reaction temperature, the feed vaporizes, at this point carbocations are formed. Carbocation is a generic term for a positive-charged carbon ion. Carbocations can be either carbonium or carbenium ions. A carbonium ion, $^{+}CH_5$, is formed by adding a hydrogen ion (H+) to a paraffin molecule. This is accomplished via direct attack of a proton from the catalyst Bronsted site. The resulting molecule will have a positive charge with five bonds to it. This can be shown by Equation (9) and (10)

$$R—CH_2—CH_2—CH_2—CH_3 + H^+ \rightarrow R—{}^{+}CH_3—CH_2—CH_2—CH_3 \quad \ldots (9)$$

$$R—{}^{+}CH_3—CH_2—CH_2—CH_3 \Rightarrow R—{}^{+}CH—CH_2—CH_2—CH_3 + H_2 \quad \ldots (10)$$

Since the carbonium ion charge formed is not stable and the acid sites on the catalyst are not strong enough to form many carbonium ions. Nearly all the cracking chemistry is carbenium ion chemistry. A carbenium ion, $R\text{-}^{+}CH_2$, can be formed directly or indirectly, direct formation of this carbenium ion comes from adding a positive charge to an olefin and the indirect formation involves formation of a carbonium ion which is unstable, hence decomposes to a carbenium ion as shown in the Equation (11)

$$R—CH{=}CH—CH_2—CH_2—CH_3 + H^+ \rightarrow R—{}^{+}CH—CH_2—CH_2—CH_2—CH_3 \quad \ldots (11)$$

(a proton at Bronsted site)

$$R—CH_2—CH_2—CH_2—CH_3 \rightarrow R—{}^{+}CH—CH_2—CH_2—CH_3 \quad \ldots (12)$$

(removal of H^- at Lewis site)

Both the Bronsted and Lewis acid sites on the catalyst generate carbenium ions. The Bronsted site donates a proton to an olefin molecule and the Lewis site removes electrons from a paraffin molecule.

Usually in most commercial units, olefins come in with the feed or are produced through thermal cracking reactions. The stability of carbocations depends on the nature of alkyl groups attached to the positive charge. The relative stability of carbenium ions as follows with tertiary ions being the most stable:

Tertiary > Secondary > Primary

One of the benefits of catalytic cracking is that the primary and secondary ions tend to rearrange to form a tertiary ion (a carbon with three other carbon bonds attached). Once formed, carbenium ions can form a number of different reactions. The nature and strength of the catalyst acid sites influence the extent to which each of these reactions occurs.

2.3.5 Hydrocracking process

Hydrocracking is a thermal process (>350˚C) in which cracking is followed by hydrogenation. Relatively high pressure (100 to 2000psi) are employed, and the overall result is usually a change in the character or quality of the products.

The wide range of products possible from hydrocracking is the result of combining catalytic cracking reactions with hydrogenation. The reactions are catalyzed by dual-function catalysts in which the cracking function is provided by silica–alumina (or zeolite) catalysts, and platinum, tungsten oxide, or nickel provides the hydrogenation function. Most of the initial reactions of catalytic cracking occur during hydrocracking, but some of the secondary reactions are prevented by the presence of hydrogen. For example, the yields of olefins and the secondary reactions that result from the presence of these materials are substantially diminished and branched-chain paraffins undergo demethanation. The methyl groups attached to secondary carbons are more easily removed than those attached to tertiary carbon atoms, whereas methyl groups attached to quaternary carbons are the most resistant to hydrocracking (Harold *et al.*, 2004).

The effect of hydrogen on naphthenic hydrocarbons is mainly that of ring scission followed by immediate saturation of each end of the fragment produced. The ring is preferentially broken at favored positions, although generally all the carbon–carbon bond positions are attacked to some extent. For example, methyl-cyclopentane is converted (over a platinum carbon catalyst) to 2-methylpentane, 3-methylpentane, and n-hexane.

Aromatic hydrocarbons are resistant to hydrogenation under mild conditions, but under more severe conditions, the main reactions are conversion of the aromatic to naphthenic rings and scissions within the alkyl side chains (Speight, 2007). The naphthenes may also be converted to paraffins.

However, poly-nuclear aromatics are more readily attacked than the single-ring compounds, the reaction proceeding by a stepwise process in which one ring at a time is saturated and then opened. For example, naphthalene is hydrocracked over molybdenum oxide–molecular catalyst to produce a variety of low weight paraffins (≤C6).

2.4 Kinetic Modeling of Catalytic Cracking

Describing the kinetic mechanism of catalytic cracking has been challenging for researchers in the field of fluid catalytic cracking; this is due to the presence of many compounds in the feedstock of FCCU. The complexity of the FCC feedstock makes it difficult to describe the kinetics at a molecular level; as a result the kinetics modeling of catalytic cracking has been traditionally based on using a lumping technique: components with similar behaviors are grouped together forming a smaller number of “pseudo” species (Affum *et al*., 2013).

There are two approaches to this lumping technique in catalytic cracking of heavy gas oil. The first method is to lump molecules in different distillation cuts “pseudo-species” and to consider chemical reactions between these lumps. These lumps are usually the feedstock and the final cracking products, like gasoline, kerosene, diesel, light cycle oil (LCO), light gases, and coke. The second approach is to lump different products based on main chemical families such as paraffins, olefins, naphthenes, and aromatics (Rajkumar *et al*., 2005).

In this respect, the first lumping model proposed was the three-lump model advanced by Weekman *et al*., (1970). The three-lump was later modified, by Yen *et al.*, (1987), proposing a more sound approach with four-lump where coke and gases were separated. A more complicated and detailed lump model (10-lumps) describing the feedstock in more detail was proposed by Jacob *et al*., (1976). The 10-lump model is of special importance to FCC model development since its rate constants do not depend, in particular, on the feedstock composition.

2.4.1 Three-lump model

The three-lump model consists of one feedstock lump (heavy gas oil or any other heavy feed) and two product lumps, gasoline and coke plus light gases. The gasoline lump contains the fraction between C5 up to the hydrocarbons with a 220^{o}C boiling temperature. The coke plus light gases lump contains in addition to coke, C_4 and lighter than C4 hydrocarbons. This model can be represented as shown in Figure 2.2:

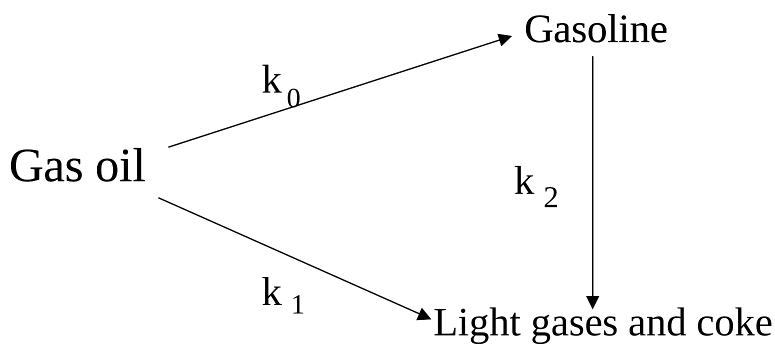

Figure 2.2: The three lump model

Since the feedstock (heavy gas oil) contains a mixture of several thousand compounds of widely different properties, a second order was suggested for cracking of HGO (Rajkumar *et al*., 2005). However, since gasoline contains a restricted range of molecular weight hydrocarbons (C5 to C12), Weekman *et al* (1970) suggested a first order reaction for gasoline cracking. This model predicted the yield of gasoline but ignored the important aspect of coke deposition on the catalyst surface.

Based on these assumptions the following equations were considered:

Gas oil cracking was represented as

$$-r_{go}=k_{T0}\varphi_1 C_{go}^{\ 2} \qquad \text{… (13)}$$

Gasoline formation was modeled as:

$$r_g=k_{T1}\varphi_1 C_{go}^{\ 2}-k_{T3}\varphi_2 C_g \qquad \text{… (14)}$$

Light gases and coke was represented as:

$$r_C=k_{T2}\varphi_1 C_{go}^{\ 2}+k_{T3}\varphi_2 C_g \qquad \text{… (15)}$$

2.4.2 Four-lump model

Introduction of the four-lump model splits the light gases plus coke lump in two separate lumps: coke and light gases and a second order conversion was assumed for the heavy gas oil cracking (Rajkumar *et al.,* 2005). The kinetic parameters were determined from riser pilot plant data and were correlated with feedstock characteristics, and operating conditions. This model is claimed to predict very effectively the coke yield for HGO cracking in FCC pilot plants and commercial units. This model can be represented as shown in Figure 2.3.

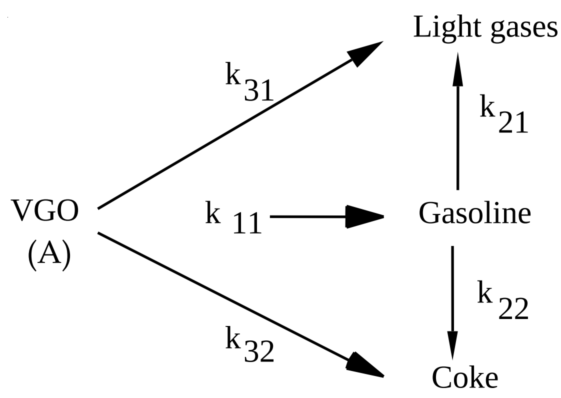

Figure 2.3: Four lump model

The rates of gasoline formation and gasoline consumption were described as,

Gas oil consumption rate

$$-r_{go} = k_{11}\varphi C_{go}^{2} \qquad \dots (16)$$

Net gasoline formation rate

$$r_{g} = k_{11}\varphi C_{go}^{2} - \varphi(k_{21} + k_{22})C_{g} \qquad \dots (17)$$

Net light gases formation rate

$$r_{lg} = k_{31}\varphi C_{go}^2 + k_{21}\varphi C_g \quad \ldots (18)$$

Coke formation rate

$$r_c = k_{32}\varphi C_{go}^2 + k_{22}\varphi C_g \quad \ldots (19)$$

Juarez *et al.*, (1999) extended the four-lump model to five lumps. These researchers further divided the gases lump into two different lumps: dry gas and LPG. Note that LPG can be formed either directly from gas oil or as a secondary product from gasoline over-cracking. On the other hand, dry gas (H_2, C_1, C_2) can be formed either directly from gas oil cracking or as a secondary product from gasoline and LPG cracking. The five-lump model can be schematically represented as shown in Figure 2.4.

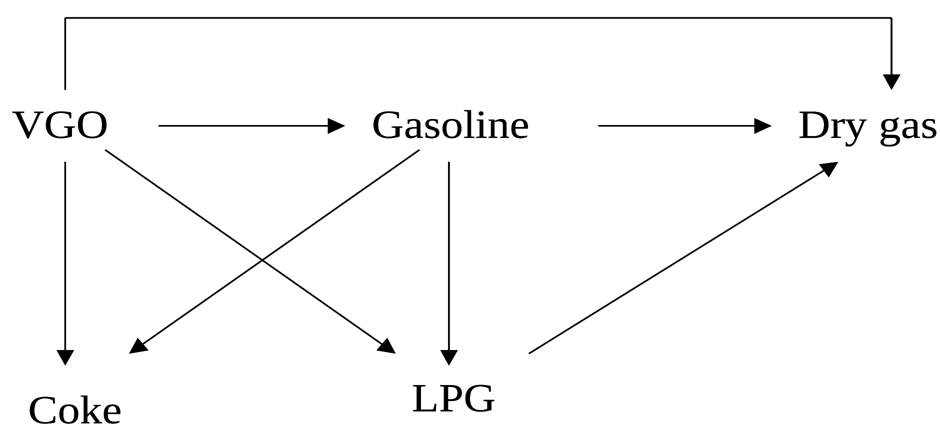

Figure 2.4: The five lump model

2.4 Cracking Catalysts

The introduction of zeolite in commercial FCC catalysts in the early1960s was one of the most significant advances in the history of catalytic cracking (Sadeghbeigi, 1995). Zeolite catalysts provided a greater profit with little capital investment. Simply stated, zeolite catalysts were and still are the biggest bargain of all time for the refiner. Improvements in catalyst technology have continued, enabling refiners to meet the demands of their market with minimum capital investment (Sadeghbeigi, 1995).

The zeolite catalysts are more active and more selective than the amorphous silica-alumina catalysts. The higher activity and selectivity translate to more profitable liquid product yields and additional cracking capacity. To take full advantage of the zeolite catalyst, refiners have revamped older units to crack more of the heavier, lower value feedstock.
FCC catalysts are in the form of fine powders with an average particle size in the range of 75 microns. A modern catalytic cracking catalyst has four major components:

- Zeolite
- Matrix
- Binder
- Filler

2.4.1 Zeolites and zeolite chemistry

Zeolites are crystalline solids structures made of silicon, aluminum and oxygen that form a framework with cavities and channels inside where cations, water and/or small molecules may reside. They are often also referred to as molecular sieves. Many of them occur naturally as minerals, and are extensively mined in many parts of the world finding applications in industry and medicine. However, most of zeolites have been made synthetically some of them made for commercial use while others created by scientists to study their chemistry. At present, there are 191 unique zeolite frameworks identified (Scott, 2003) and over 40 naturally occurring zeolite frameworks are known.

Zeolite Y, with a faujasite framework or structure, is the key ingredient of the FCC catalyst. It provides product selectivity and much of the catalytic activity. The catalyst performance largely depends on nature and quality of zeolite. Understanding its structure, types and catalytic mechanism helps in predicting the choice of catalyst to produce the desired yields.

Zeolites are crystalline, micro-porous hydrated alumino-silcate minerals that contain alkaline and alkaline earth metals. They have open 3D framework structures built of SiO_4 and AlO_4 tetrahedra linked to each other by sharing all the oxygen atoms to form regular intra-crystalline cavities and channels of molecular dimensions. A defining feature of zeolites is that their frameworks are made up of 4-coordinated atoms forming tetrahedra. These tetrahedra are linked together by their corners and make a rich variety of beautiful structures.

The typical zeolite consists of silicon and aluminum atoms that are tetrahedrally coordinated by four oxygen atoms. Silicon is in a +4 oxidation state; therefore, tetrahedral containing silicon is neutral in charge. In contrast, aluminum is in a +3 oxidation state. This indicates that each tetrahedron containing aluminum atom has a net charge of -1 which must be balanced by a positive ion. This ionic site accounts for the catalytic activity of zeolite.

An alkaline solution preferably sodium hydroxide is usually used for preparation of zeolites. The sodium ion is used to neutralize the zeolite framework which is negatively charged. This zeolite is called soda Y or NaY. The NaY is not hydrothermally stable because of the high sodium content. Ammonium ion is usually used to displace the sodium, and then during calcination at high temperatures of about 600˚C, the ammonium ion is vaporized. The resulting acid sites are called the Bronsted acid sites (Sadeghbeigi, 1995). The Bronsted acid sites can further be exchanged with rare earth materials such as cerium and lanthanum to enhance their strengths. The zeolite activity comes from these sites.

2.4.2 Zeolite properties

Zeolite must be able to withstand and retain their catalytic properties from the hostile conditions of the FCC operation such as high attrition during fluidization and exposure to high temperatures in the regenerator unit. The properties of zeolites play significant role in the overall performance as they influence catalyst response to changes in the FCC operation. The reactor and regenerator can cause significant changes in the chemical and structural composition of the zeolite.

Several analytical tests are carried out to determine zeolite properties. These tests will provide information about the strength, type, number and distribution of acid sites. Unit cell size, rare earth level and sodium content are one of the tests that describe the behavior of zeolite (Sadeghbeigi, 1995).

- ***Unit cell size***

The unit cell size (UCS) is a measure of aluminum sites or the total potential acidity per unit cell. Unlike the silicon atoms, the negatively charged aluminum atoms are source of active sites in the zeolite. The UCS is related to the number of aluminum atoms per cell, N_{Al} by

$$N_{Al} = 111 \times (UCS - 24.215)$$

The number of silicon atoms per cell is $N_{si} = 192 - N_{Al}$

The silicon to aluminum atomic ratio, SAR of the zeolite can be determined either from the above two equations or from a correlation such as the one shown in Figure 2.5

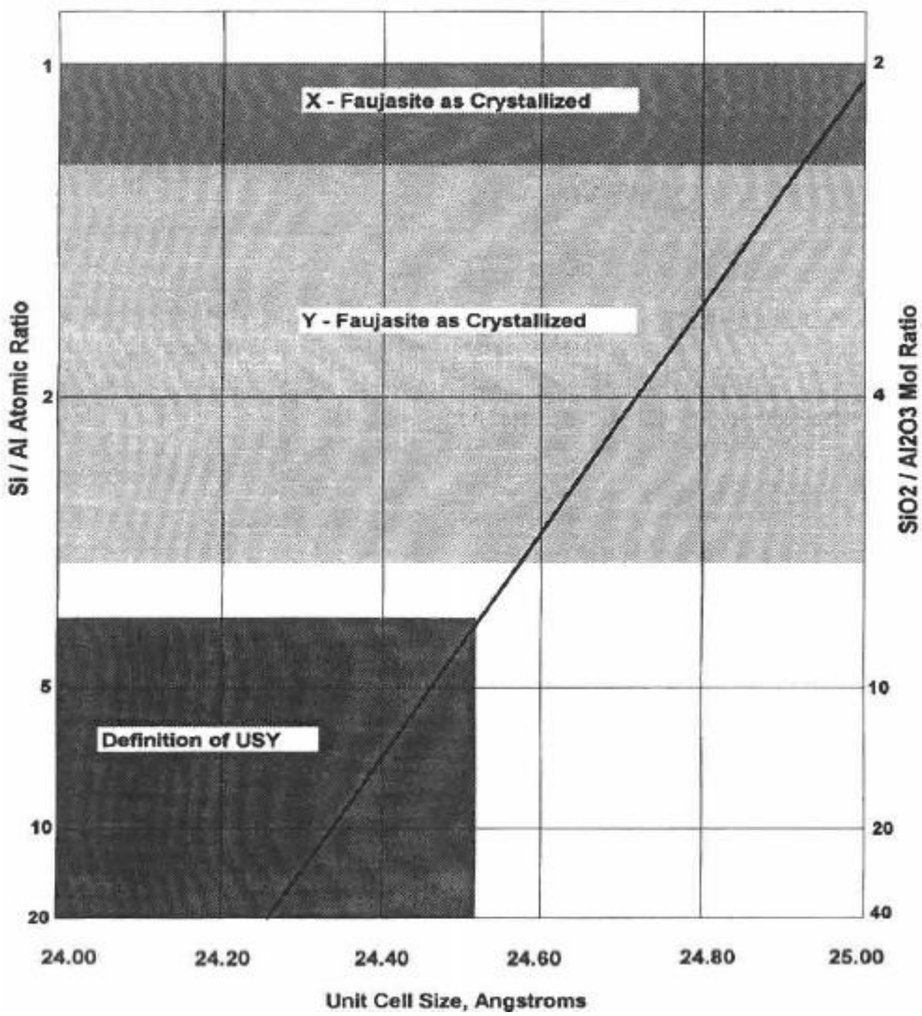

Figure 2.5: Silica-alumina ratios versus zeolite unit cell size (Sadeghbeigi, 1995).

The zeolite acidity level can also be indicated by the unit cell size, UCS. This is due to the size of aluminum ion being larger than the silicon ion, as the UCS decreases, the acid sites become farther apart. The strength of the acid sites is determined by the extent of their isolation from the neighboring acid sites (Bruce *et al*., 1979). The closer the acid sites, the less stable the structure of zeolite becomes. Acid distribution of the zeolite is a fundamental factor affecting zeolite activity and selectivity. Additionally, the UCS measurement can be used to indicate octane potential of the zeolite. A lower UCS presents fewer active sites per unit cell. The fewer acid sites are farther apart and, therefore, inhibit hydrogen transfer reactions, which in turn increase gasoline octane as well as the production of C3 and lighter components (Sadeghbeigi, 1995). The octane increase is due to a higher concentration of olefins in the gasoline.

A freshly manufactured zeolite has a relatively high UCS in the range of 24.50°A to 24.75°A. The thermal and hydrothermal environment of the regenerator extracts alumina from the zeolite structure and, therefore, reduces its UCS. The final UCS level depends on the rare earth and sodium level of the zeolite. The lower the sodium and rare earth content of the fresh zeolite, the lower UCS of the equilibrium catalyst.

- ***Rare earth level***

Rare earth (RE) elements serve as a "bridge" to stabilize aluminum atoms in the zeolite structure. They prevent the size, aluminum atoms from separating from the zeolite lattice when the catalyst is exposed to high temperature steam in the regenerator. A fully rare-earth-exchanged zeolite equilibrates at a high UCS, whereas a non-rare-earth zeolite equilibrates at a very low UCS in the range of 24-25°A (Sadeghbeigi, 1995). All intermediate levels of rare-earth-exchanged zeolite can be produced. The rare earth increases zeolite activity and gasoline selectivity with a loss in octane (Sadeghbeigi, 1995). The octane loss is due to promotion of hydrogen transfer reactions. The insertion of rare earth maintains more and closer acid sites, which promotes hydrogen transfer reactions. In addition, rare earth improves thermal and hydrothermal stability of the zeolite. To improve the activity of a USY zeolite, the catalyst suppliers frequently add some rare earth to the zeolite.

- ***Sodium content***

The source of sodium on the catalyst can result from zeolite during its manufacture or from the FCC feedstock. Sodium decreases the hydrothermal stability of the zeolite; consequently it is important for the fresh zeolite to contain very low amounts of sodium. It also reacts with the zeolite acid sites to reduce catalyst activity. Since sodium is mobile, its ions tend to neutralize the strongest acid sites in the regenerator. In a dealuminated zeolite, where the UCS is low 24.22°A to 24.25°A, the sodium can have an adverse effect on the gasoline octane (Figure 2.6). The loss of octane is attributed to the drop in the number of strong acid sites.

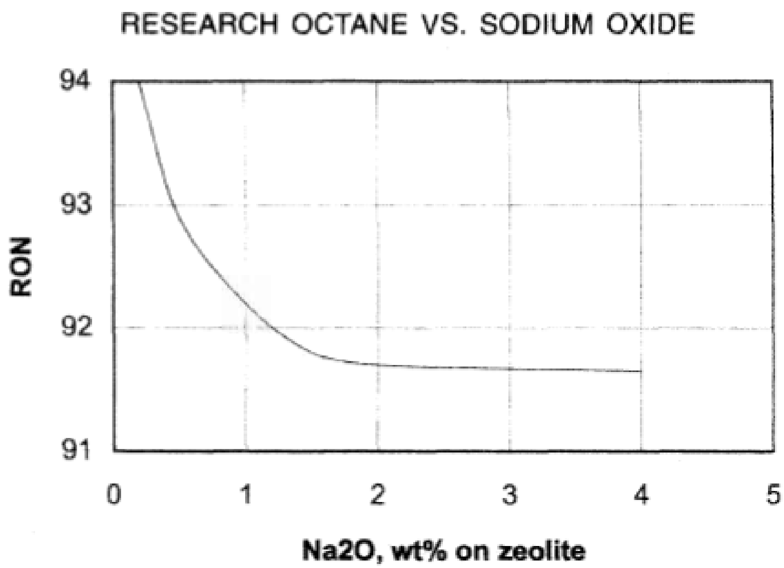

Figure 2.6: Effects of soda on motor and research octanes: motor octane versus sodium oxide, (Sadeghbeigi, 1995).

The proper way to compare sodium is the weight fraction of sodium in the zeolite. This is because FCC catalysts have different zeolite concentrations. UCS, rare earth, and sodium are just three of the parameters that are readily available to characterize the zeolite properties. They provide valuable information about catalyst behavior in the catalytic cracker.

2.4.3 Matrix, binders and fillers

The term matrix can have different meaning depending on the context in which it is used. For some purposes, matrix can refer to components of the catalyst other than the zeolite. In others, matrix is a component of the catalyst aside from the zeolite having catalytic activity. Yet for others, matrix can be referred to as the catalyst binder. More general, matrix means components of the catalyst other than zeolite and the term active matrix means the component of the catalyst other than zeolite having catalytic activity.

The main source for an active matrix is usually alumina with most active matrices used in FCC catalysts being amorphous. However, some of the catalyst suppliers incorporate a form of alumina that also has a crystalline structure. Active matrix contributes significantly to the overall performance of the FCC catalyst as it provides a larger pore size for cracking of larger molecules that cannot access the pore sizes of the active ingredient(zeolite) hence reduces diffusional constraints. Zeolites are too small to allow diffusion of the large molecules to the cracking sites. An effective matrix must have a porous structure to allow diffusion of hydrocarbons into and out of the catalyst.

The primary cracking of the hydrocarbon occurs on the active matrix. The acid sites located in the catalyst matrix are not as selective as the zeolite sites, but are able to crack larger molecules that are hindered from entering the small zeolite pores. The main contribution of the active matrix is that it pre-cracks heavy feed molecules for further cracking at the internal zeolite sites. The result is a synergistic interaction between matrix and zeolite, in which the activity attained by their combined effects is usually greater than the sum of their individual effects.

An active matrix can also serve as a trap to catch some of the vanadium and basic nitrogen. The high boiling fraction of the FCC feed usually contains metals and basic nitrogen that poison the zeolite. One of the advantages of an active matrix is that it protects the zeolite from being deactivated prematurely by these impurities(Sadeghbeigi, 1995).

While having the active matrix with the active ingredient, fillers are also incorporated into the catalyst to dilute its activity. Kaolin [$Al_2(OH)_2.Si_2O_5$] is the most common clay used in the FCC catalyst (Bruce *et al*., 1979). The binder serves as a glue to hold the zeolite, matrix, and filler together. Binder may or may not have catalytic activity. The importance of the binder becomes more prominent with catalysts that contain high concentrations of zeolite.

As a result the functions of the binders and fillers are to provide physical integrity (density, attrition resistance, particle size distribution, etc.), heat transfer medium, and a fluidizing medium in which the more important and expensive zeolite component is incorporated.

2.4.4 Natural and synthetic zeolites

There are two kinds of zeolite, natural and synthetic zeolites. Natural zeolites are obtained from natural ore bodies. They are mainly found in the voids of basalt and volcanic rocks (Ahmed *et al.*, 2007). They are formed as a result of the chemical reaction between volcanic ash and alkaline water. The natural zeolite structure has more acid resistant so it does not break down in mildly acid environment. Therefore the natural zeolites are broadly used in the agricultural industry. Since the discovery of molecular sieve and ion exchange properties, they have been used as molecular sieve adsorbents in the natural gas industry, ammonia industry and water treatment. Natural zeolites have also found applications in paper, cements and concrete industries, which represent the major volume applications for natural zeolites. The examples of natural zeolites are Chabazite, erionite, mordenite and gmelnite etc.

Zeolites can be synthesized from reactive starting materials such as freshly coprecipitated gels (sodium silicate and sodium aluminate), or amorphous solids (kaolinite, perlite, halloysite, etc.) by controlling the condition to form uniform growth of crystal such as

a) Relatively high pH introduced in the form of an alkali metal hydroxide or other strong base

b) Low temperature hydrothermal conditions with concurrent low autogeneous pressure at saturated water vapor or

c) A high degree of super-saturation of the components of the gel leading to the nucleation of a large number of crystals (Ahmed *et al.*, 2007).

The formation of zeolite can be influenced by several factors such as

a) The nature of the reactants and their pretreatment.

b) The process in which the reactant mixture is made and pretreated and its overall chemical composition.

c) Homogeneity or heterogeneity of the mixture.

d) pH of the mixture.

e) Low temperature aging of gels.

f) Seeding.

g) Addition of special additive or

h) Temperature and pressure.

The examples of synthetic zeolites are zeolite A, X, Y and L

The structural formula of zeolite is based on the crystallographic unit cell, the smallest unit of structure, represented as (Ahmed *et al.*, 2007).

$$M_{x/n}\left[(AlO_2)_x(SiO_2)_y\right].wH_2O$$

where M is an alkali or alkaline earth cation, n is the valence of the cation, w is the number of water molecules per unit cell, x and y are the total number of tetrahedra per unit cell, and the ratio y/x usually has values of 1 to 5. In the case of the high silica zeolite, y/x can be ranging from 10 to 100 (Ahmed *et al*., 2007).

Zeolites primary structures are tetrahedra of SiO_4 and AlO_4 shown in Figure 2.7. Each sub-unit contains the pores and cavities within the frameworks, which were called secondary building units (SBUs) and illustrated in Figure 2.8. The SBUs can be simple arrangements of tetrahedral such as four, six, or eight-membered ring or more complex structure.

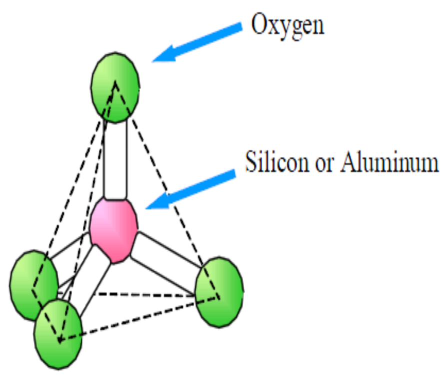

Figure 2.7: Primary building unit of zeolite structure

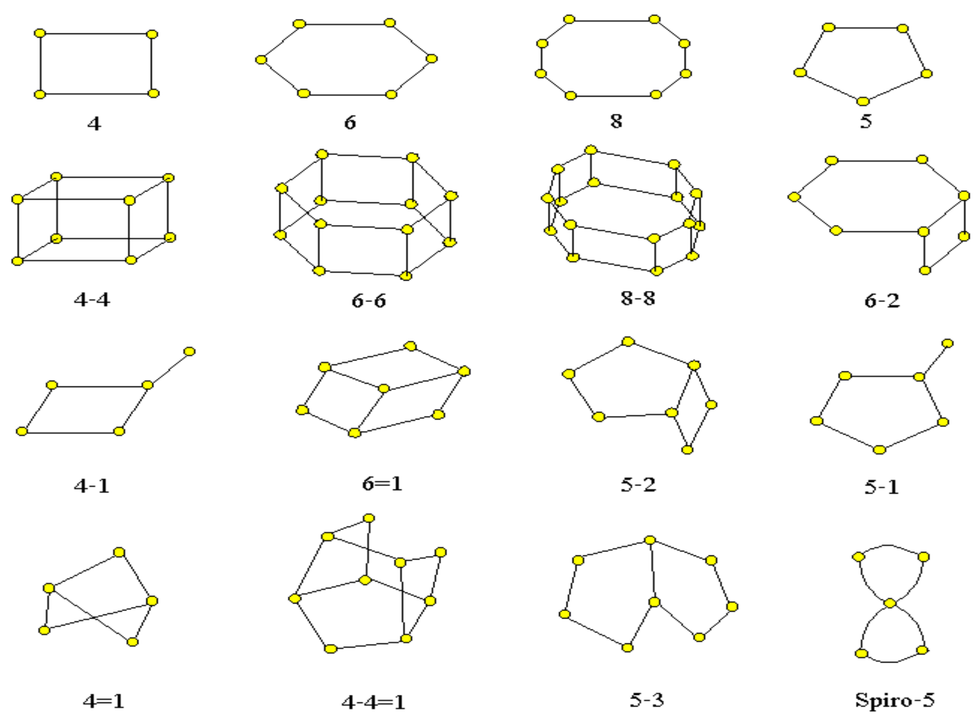

Figure 2.8: Secondary Building Units (SBUs) of zeolite structure

2.4.5 Zeolite Y

Zeolite Y exhibits the faujasite (FAU) structure as shown in Figure 2.9. It has a 3-dimensional pore structure with pores running perpendicular to each other in the x, y, and z planes, and is made of secondary building units 4, 6, and 6-6 (Niken, 2011). The pore diameter is large at 7.4Å since the aperture is defined by a 12 member oxygen ring, and leads into a larger cavity of diameter 12Å. The cavity is surrounded by ten sodalite cages (Figure 2.10) connected on their hexagonal faces. Zeolite Y has a void volume fraction of 0.48, with a Si/Al ratio of 2.43 and it thermally decomposes at 793ºC (Niken, 2011).

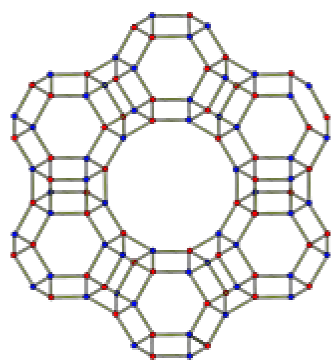

Figure 2.9: Crystal structure of zeolite Y

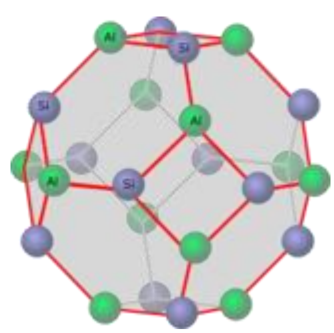

Figure 2.10: Sodalite cage of zeolite Y

CHAPTER THREE

MATERIALS AND METHODS

3.1 INTRODUCTION

This chapter presents the step by step procedure for the catalytic cracking of heavy gas oil into liquid products which are then analyzed using gas chromatography. The catalytic cracking set-up shown in Section 3.2.3 tries to mimic the conventional fluid catalytic cracking unit in the refinery in terms of fluidizing the catalyst. The equipment used in this set-up such as the tube furnace, nitrogen gas cylinder and the chiller were all calibrated to reduce systematic error.

The heavy gas oil used in this study was obtained from Kaduna Refinery and Petrochemical Company. The catalysts used in the cracking process are of three categories: synthesized zeolite Y, 25% zeolite ZSM-5 blended with 75% zeolite Y and commercial zeolite Y.

3.2 MATERIALS

Sample of heavy gas oil (4 liters)

Nitrogen gas

Chemicals (GC Standards): C6, C7, C8 C8=, C10, C10=, C12, C12=, C14, C14=, C18, C18=, C20, C22, C24, C28

Catalysts (Commercial zeolite Y, synthesized zeolite Y and zeolite Y/ZSM-5)

3.3 General Description of Equipment

3.3.1 Determination of condensation temperature

Chiller Thermo Circulator (Churchill condenser) was used to achieve condensation of the cracked gas oil vapor to an appreciable amount. The chiller outlet was connected to the set-up and a certain amount of product was collected after condensation of the product took place, the condensation temperature and remark on the quantity of condensed product were recorded as shown in Table 3.1

Table 3.1: Determination of outlet temperature of the chiller

Inlet temperature, ˚C	Outlet temperature, ˚C	Remark
26	18	No droplets
26	12	Insignificant droplets
26	5	Significant droplets

Therefore, for the purpose of using gas chromatograph to analyze the product collected, the chiller outlet temperature was set to 5^{o}C for proper condensation to take place and significant droplet collection for analysis. Also the chiller was switched on; and allowed to work for about an hour before cracking of the heavy gas oil was started.

3.3.2 Catalyst pretreatment system

The catalyst pretreatment system consists of the tube furnace, which represents or mimicked the reactor as found in the FCC unit. The tube furnace temperature gauge was graduated up to 1200^{o}C. The catalyst pretreatment involved heating the catalyst to the reaction temperature which was varied from 500^{o}C to 590^{o}C for 30min before the gas oil vapor was introduced. The silica-glass tube in the furnace, which served as the reactor, contained the catalyst, and nitrogen gas was used to fluidize the catalyst as well as pushing the oil gas vapor through the reactor.

3.2.3 Catalytic cracking system

The system here consisted of all the units assembled together as shown in Figure 3.1. It consisted of the heating mantle, reactor, nitrogen gas cylinder and condenser. 40ml of the heavy gas oil sample was heated to its boiling point, 320^{o}C and the vapor formed was channeled into the reactor (consisting of the silica glass tube which contained the catalyst as the heat required by the reaction supplied by the tube furnace).

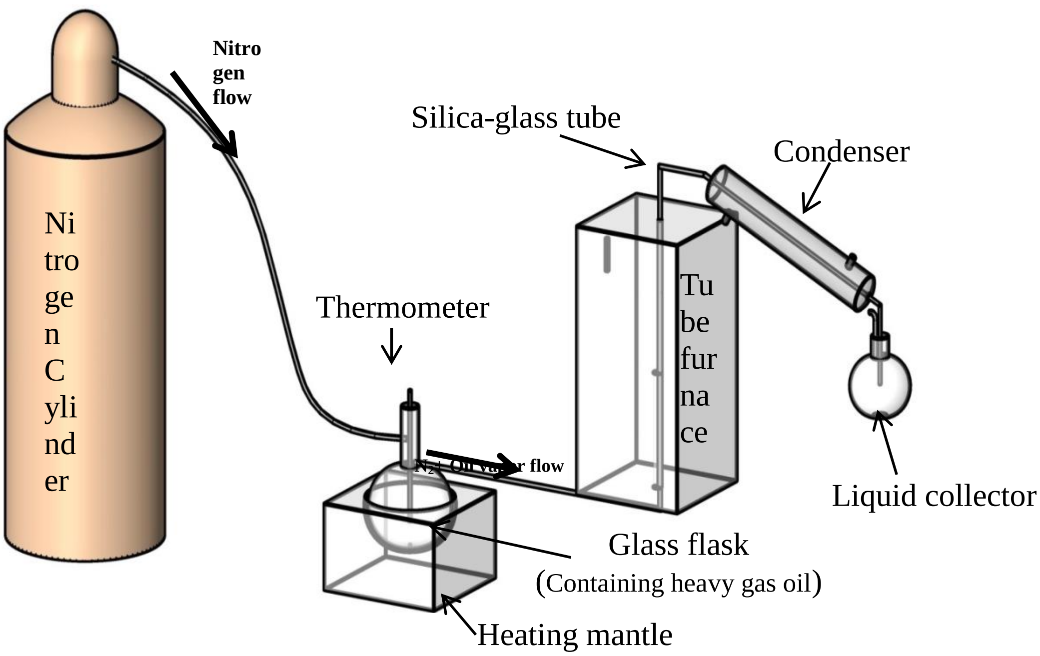

Figure 3.1: Test rig for fluidized bed catalytic cracking of HGO

The first run involved setting the tube furnace to 500^{o}C. The silica-glass tube contains 0.2g of synthesized zeolite Y (weight of the catalyst was kept constant throughout the experiment). The catalyst was kept fluidized by flow of nitrogen gas at a gauge pressure of 1psi. The catalyst was allowed to attain a uniform steady temperature (500^{o}C) for 30 minutes after which the gas oil vapor was introduced with the hot catalyst. The flow of nitrogen plus gas oil vapor was stopped after 30sec.

The catalyst cracked the heavy gas oil as it came in contact with the hot catalyst, the product formed was made to pass through the condenser which condensed the liquid component of the cracked gas oil and the gaseous component was allowed to escape to the vent. The liquid product obtained was then analyzed using gas chromatograph.

The experiment was repeated with different reaction time of 1, 2, and 3 minutes) for flow of the nitrogen plus gas oil vapor at the same temperature of the catalyst, 500^{o}C.

The experiment above was repeated with different temperatures of the catalyst at 530^{o}C, 560^{o}C and 590^{o}C and reaction time of 0.5, 1, 2, and 3min at each temperature.

The same procedure was repeated for a commercial zeolite Y catalyst and zeolite Y/ZSM-5.

3.3.4 Chromatographic Analysis

Reaction product composition was determined by gas chromatographic analysis (Agilent Technologies 7820A Gas Chromatography System) at Hydrochrom Resources Limited, Ikeja, Lagos State.

Table 3.2: Experimentalconditions for the fluidized catalytic cracking of HGO using zeolite Y and zeolite Y/ZSM-5 blend catalysts

Temperature, ˚C	Contact time, min.			
500	0.5	1.0	2.0	3.0
530	0.5	1.0	2.0	3.0
560	0.5	1.0	2.0	3.0
590	0.5	1.0	2.0	3.0

Data obtained from gas chromatograph was used to evaluate conversionusing Equation 3.1.

$$conversion, X = \frac{volume\ of\ feed - volume\ of\ residual\ feed}{volume\ of\ feed} \qquad \ldots(3.1)$$

CHAPTER FOUR

RESULTS AND DISCUSSION

The calibrations of the equipment used are presented in this chapter. The conditions of operating the catalytic cracking system was derived from these calibrations such as flow rate of nitrogen gas with the corresponding pressure gauge and the temperature for condensing the vapor products to liquids.

The results obtained from the gas chromatography are also reported here, the data are used for evaluating the conversion of the heavy gas oil, yield of the kerosene and diesel and some kinetic parameters are also evaluated from these results.

4.1 Calibration of the Flow Rate of Nitrogen Gas

The calibration of the nitrogen flow gauge was necessary to determine the pressure required to fluidize a given weight of the catalyst packed in the silica glass tube. The following result was obtained with each remark as to fluidization. With a particular pressure of nitrogen gas, a gas flow meter was used to measure the corresponding flow rate of the gas and the values are tabulated as shown in Table 4.1.

Table 4.1: Nitrogen gas flow rate determination with its corresponding gauge pressure

Nitrogen gas flow rate, scfh	Nitrogen gas pressure, psi
4.0	0.5
7.0	1.0
9.0	1.5

It can be observed from Tables 4.2 to 4.4 that the weight of the catalyst has a significant effect in fluidization with a given flow rate of nitrogen gas. Hence from this calibration, a constant weight (0.2g) of each catalyst was used throughout the experiment sincethere was significant fluidization of this weight of catalyst as shown in Table 4.5.

Table 4.2: Effect of fluidization with 1.0g of Zeolite Y catalyst

Nitrogen flow rate, schf	Fluidization	Remark
4.0	None	Causing damping of the catalyst
7.0	None	Pressure build up within the system
9.0	None	Pushes the fibre wool seal

Table 4.3: Effect of fluidization with 0.5g of Zeolite Y catalyst

Nitrogen flow rate, schf	Fluidization	Remark
4.0	None	Pressure build up within the system
7.0	None	Pressure build up within the system
9.0	None	Pushes the fibre wool seal

Table 4.4: Effect of fluidization with 0.2g of Zeolite Y catalyst

Nitrogen flow rate, schf	Fluidization	Remark
4.0	None	Little fraction of the catalyst is fluidized
7.0	None	Significant fluidization observed
9.0	None	Pushes the fibre wool seal

From Tables 4.2 to 4.4, it can be concluded that significant fluidization was observed at a nitrogen flow rate of 7.0schf. This flow rate was maintained throughout the catalytic cracking process.

4.2 Evaluation of Concentration of Hydrocarbon Molecules

C_{14}, C_{16}, $C_{14=}$ and $C_{16=}$were used to represent the kerosene range while C_{20}, C_{22}, C_{24} and C_{28} represented the diesel range, while C_6, C_7, C_8, C_{10}, C_{12}, $C_{10=}$ and $C_{12=}$were used to represent the gasoline range.

Figures 4.1 to 4.4show the calibration of the gas chromatograph used for the analysis and from these plots the concentration of the individual components was evaluated.

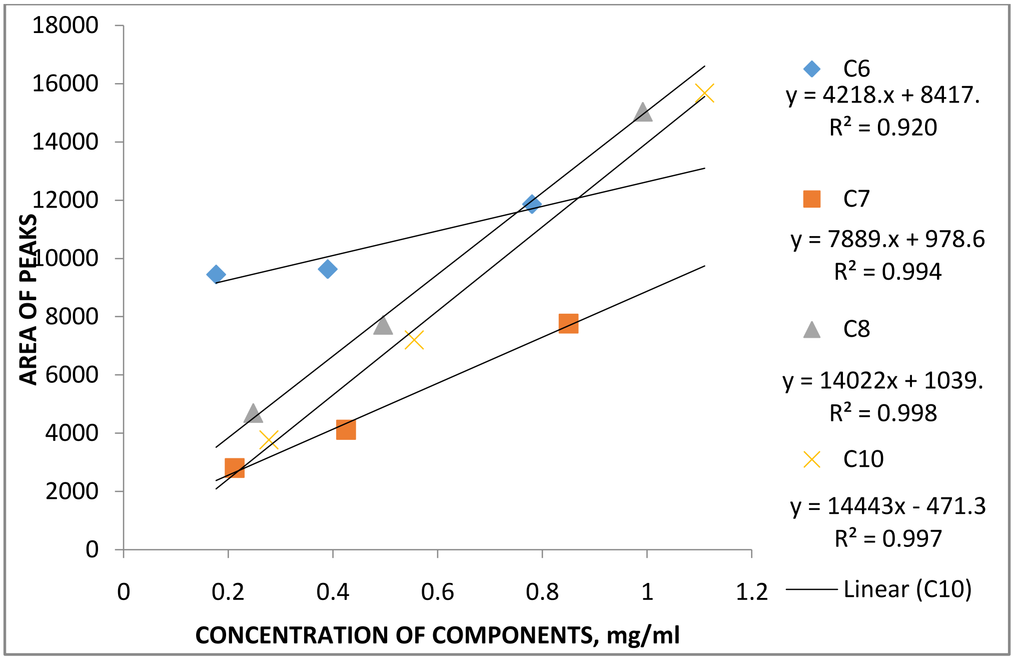

Figure 4.1: Linear dilution of standards C6, C7, C8 and C10

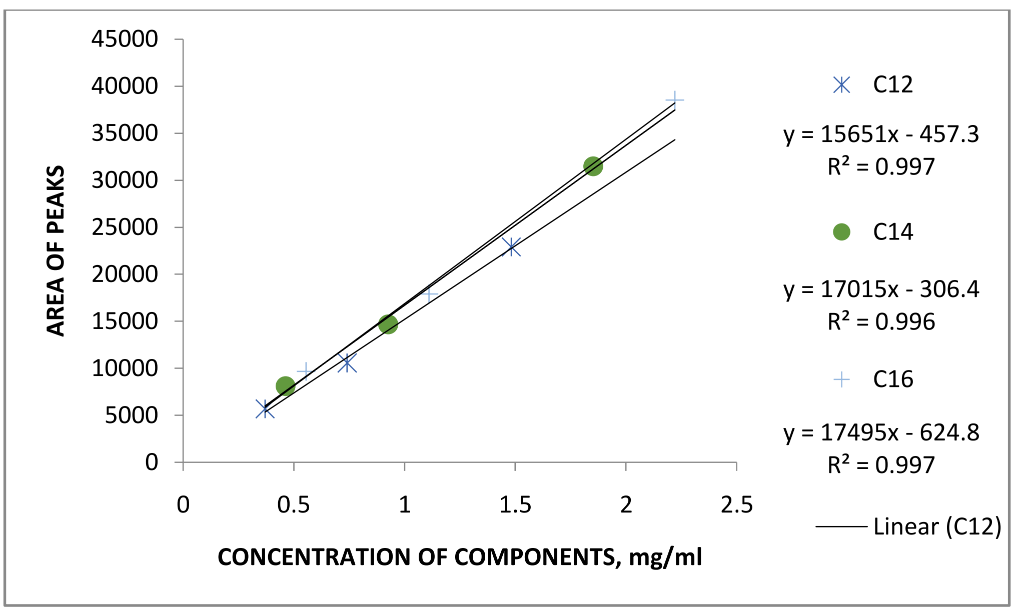

Figure 4.2: Linear dilution of standards C12, C14 and C16

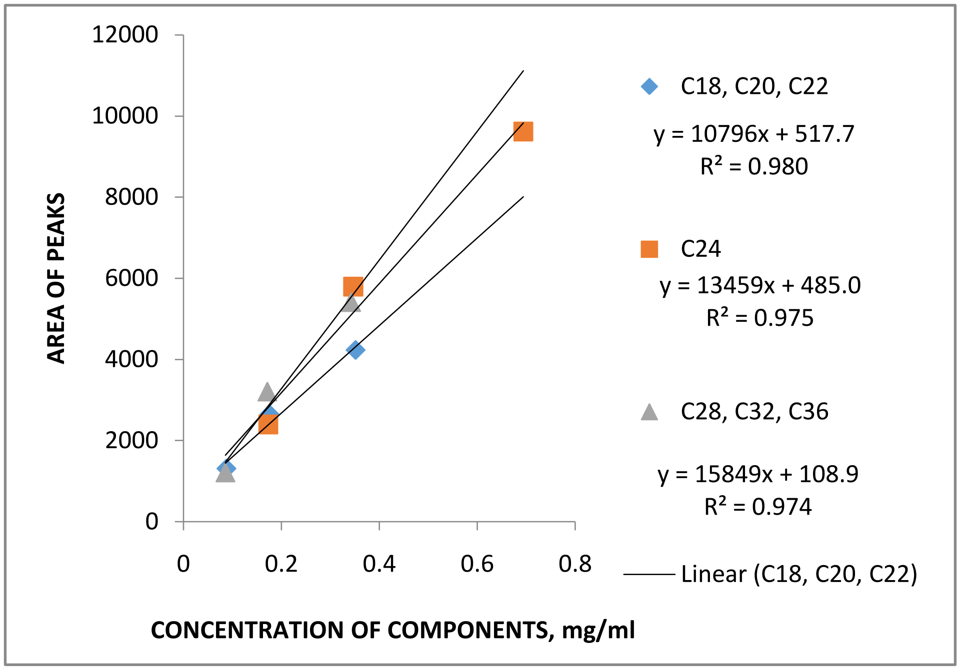

Figure 4.3: Linear dilution of standards C18, C20, C22, C24, C28, C32 and C36

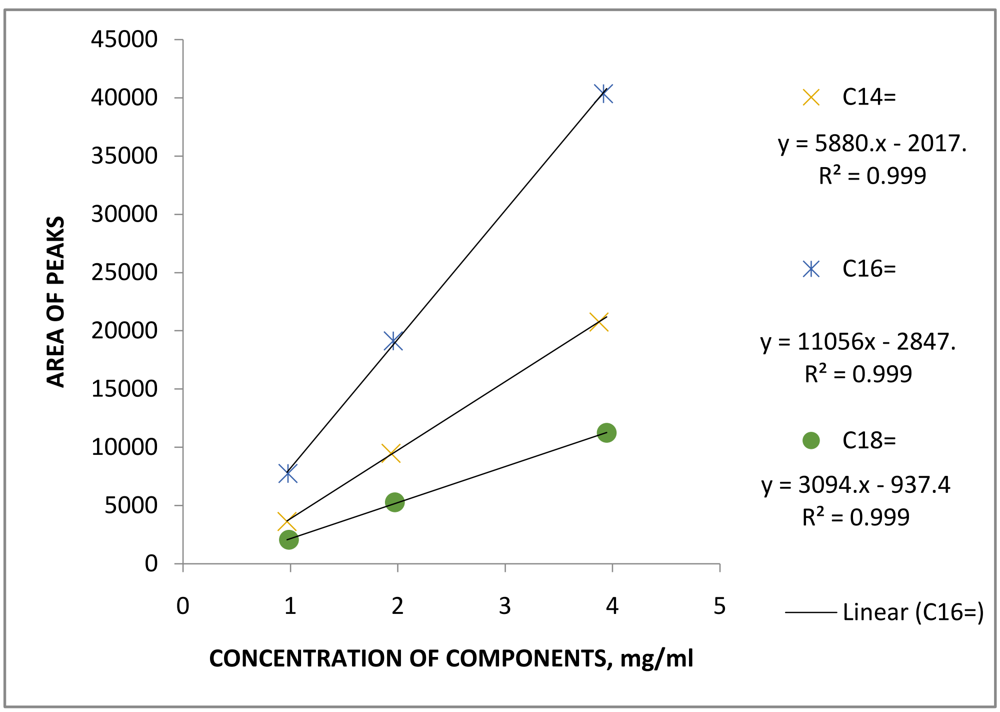

Figure 4.4: Linear dilution of standards C14=, C16=, and C18=

From Figures 4.1 to 4.4, each equation of line represented a particular component, the equivalent concentration of these components were therefore evaluated from this equations.

4.3 Simple Kinetic Model of Catalytic Cracking

The kinetic model adopted in this work was the four-lumpedmodel. This was to allow for easy studies, similar components were grouped into four lumps. The kinetics was based on the heavy gas oil conversion using Equation 3.1. The four-lumped model is shown in Figure 4.5.

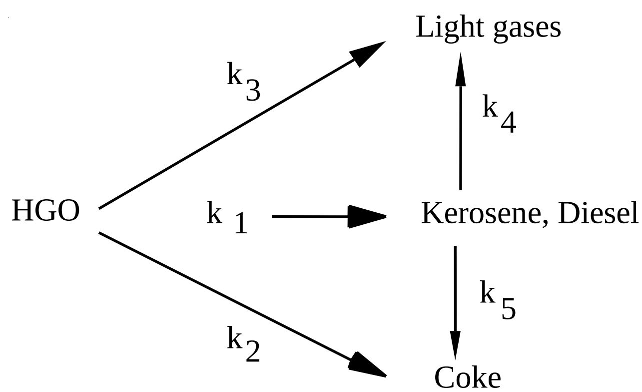

Figure 4.5: Four-lumped model adopted

In this work, the path for the conversion of heavy gas oil to kerosene and diesel were studied, hence the value of the rate constant, k_1 was evaluated.

In order to determine the order of the cracking process, the experimental data had been correlated in terms of simple kinetic models by plotting $\ln\left(\frac{1}{1-X}\right)$ and $\ln\left(\frac{X}{1-X}\right)$ against time to check for first order or second order kinetics (Chaohe *et al.*, 1997).

4.3.1 Catalytic cracking using synthesized zeolite Y

As shown in Figures 4.6 to 4.9, it was found that the first order plot bestdescribedthe kinetics of catalytic cracking of heavy gas oil using the synthesized zeolite Y with a high correlation coefficient, the correlation coefficient drops with increase in temperature, this may be attributed to deviation of the kinetics from the first order kinetics , John *et al*., (1993) reported pseudo-first order kinetics for catalytic cracking chemistry and Chaohe *et al*. (1997) investigated the reaction mechanism of hydrocracking and found that first order kinetics best described the experimental data.

The first order kinetics using the synthesized zeolite Y was an indication of one of the acid sites contributing more to the catalytic cracking of the heavy gas oil and the acid site responsible would be the Bronsted acid sites as these sites were present as a result of activation of the zeolite Y catalyst during its preparation.

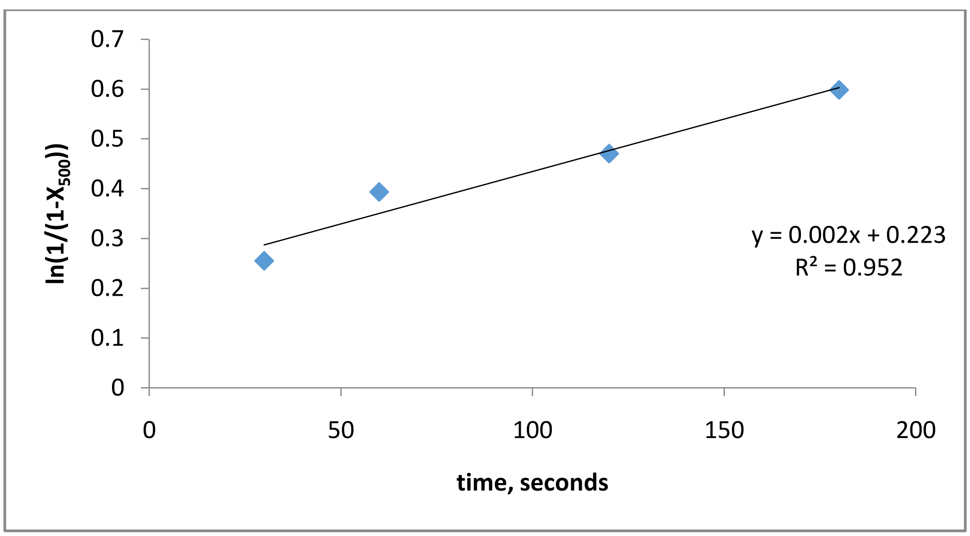

Figure 4.6: Testing first order model for synthesized zeolite Y at 500˚C

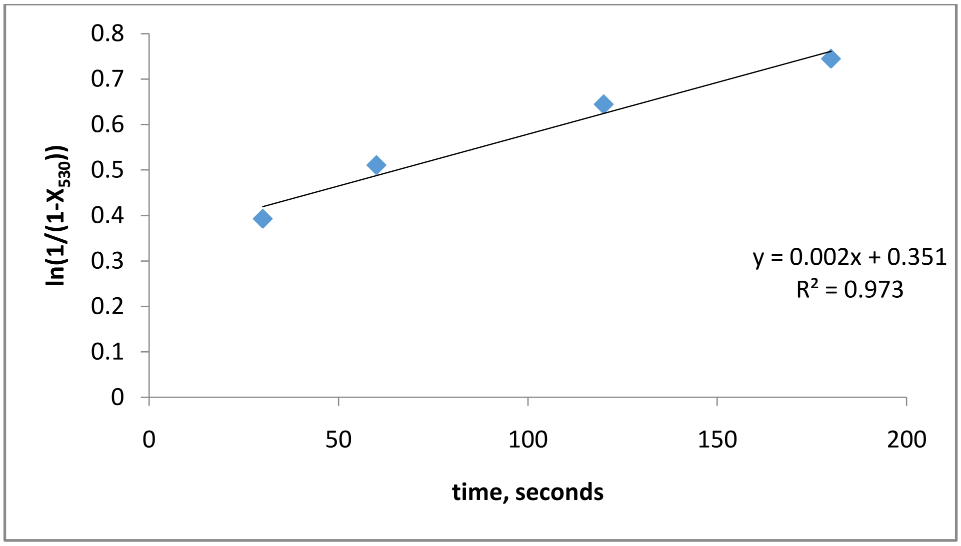

Figure 4.7: Testing first order model for synthesized zeolite Y at 530˚C

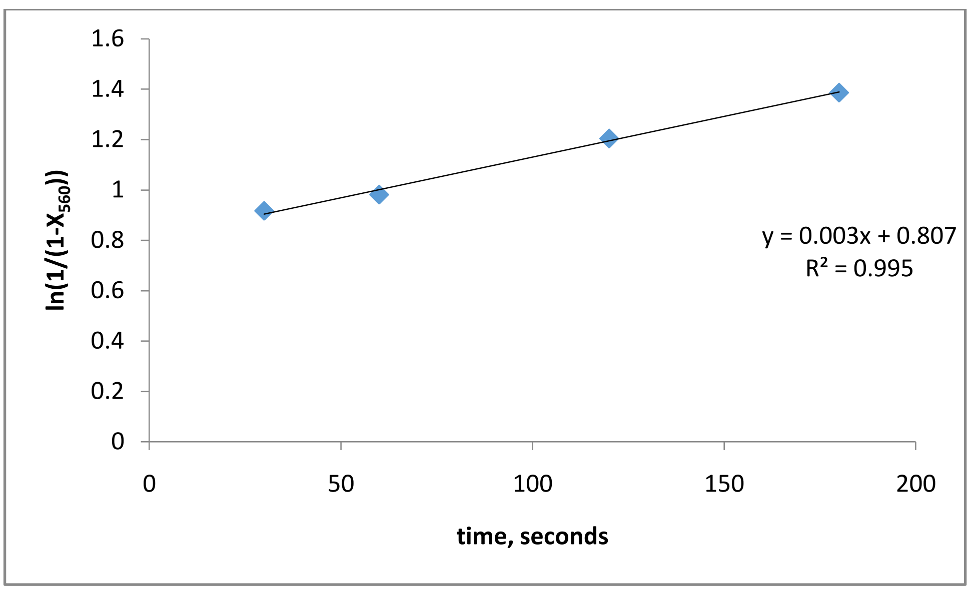

Figure 4.8: Testing first order model for synthesized zeolite Y at 560˚C

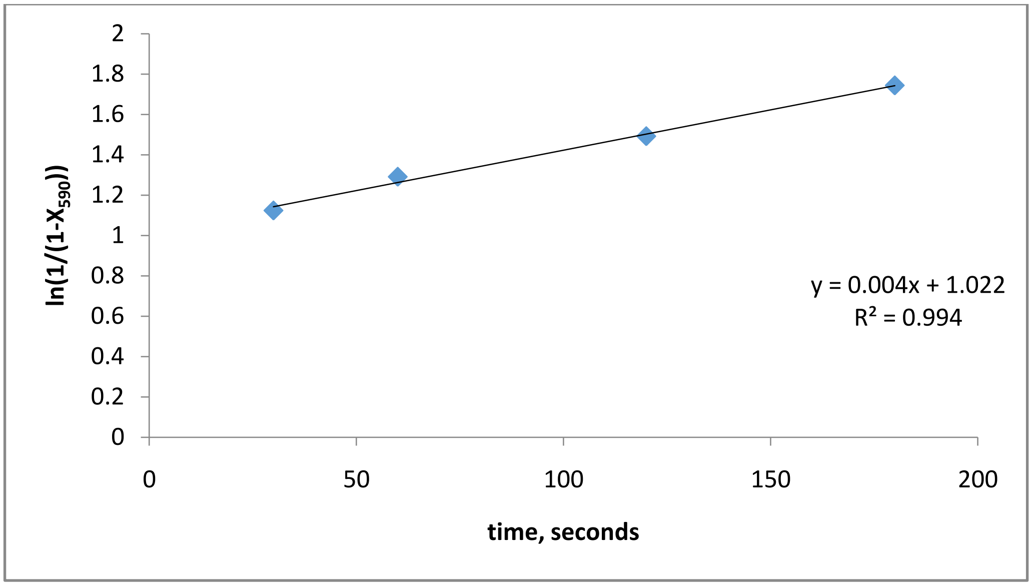

Figure 4.9: Testing first order model for synthesized zeolite Y at 590˚C

4.3.2 Catalytic Cracking Using Commercial Zeolite Y

Testing the kinetics of the catalytic cracking reaction using the commercial zeolite Y with the first order plot showed that the first order kinetics could notadequately describe the kinetics which is later shown in the Arrhenius plot, with a very poor correlation coefficient of 0.5897. Hence a further test using the second order kinetics on the experimental data was done. The first order plots are shown in Figures 4.10 to 4.13

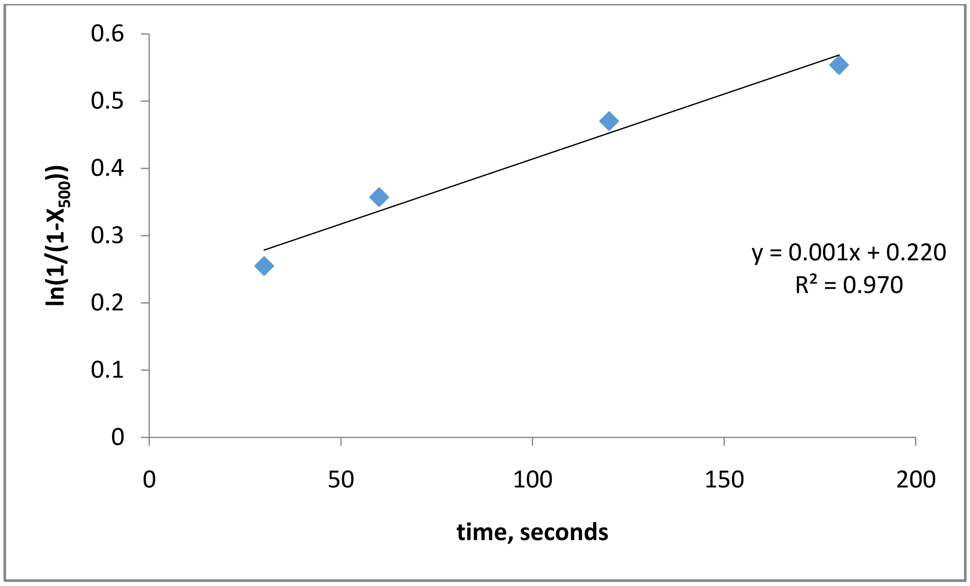

Figure 4.10: Testing first order model for commercial zeolite Y at 500˚C

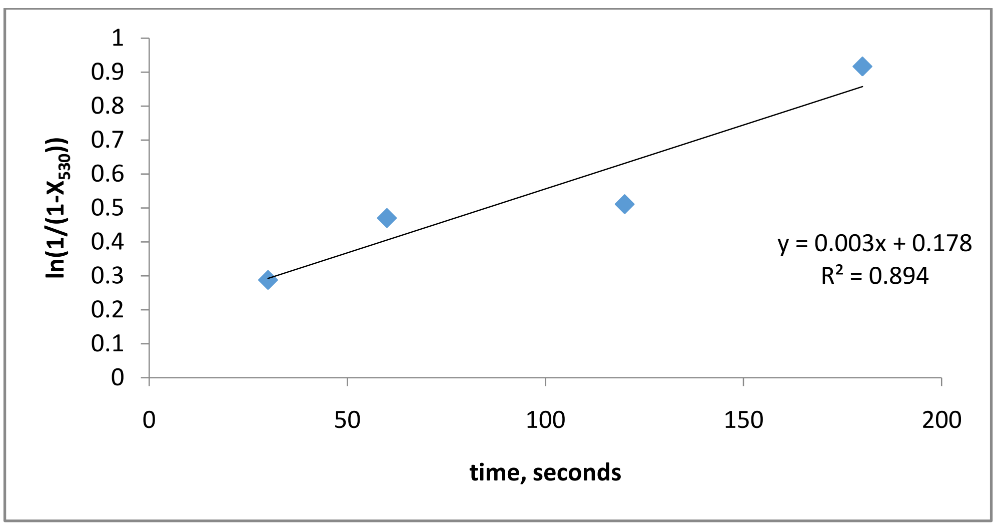

Figure 4.11: Testing first order model for commercial zeolite Y at 530˚C

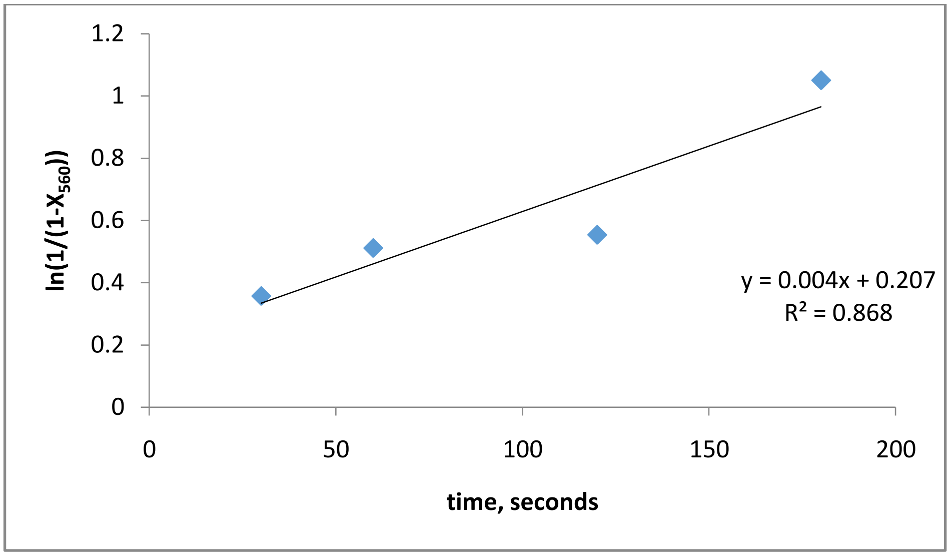

Figure 4.12: Testing first order model for commercial zeolite Y at 560˚C

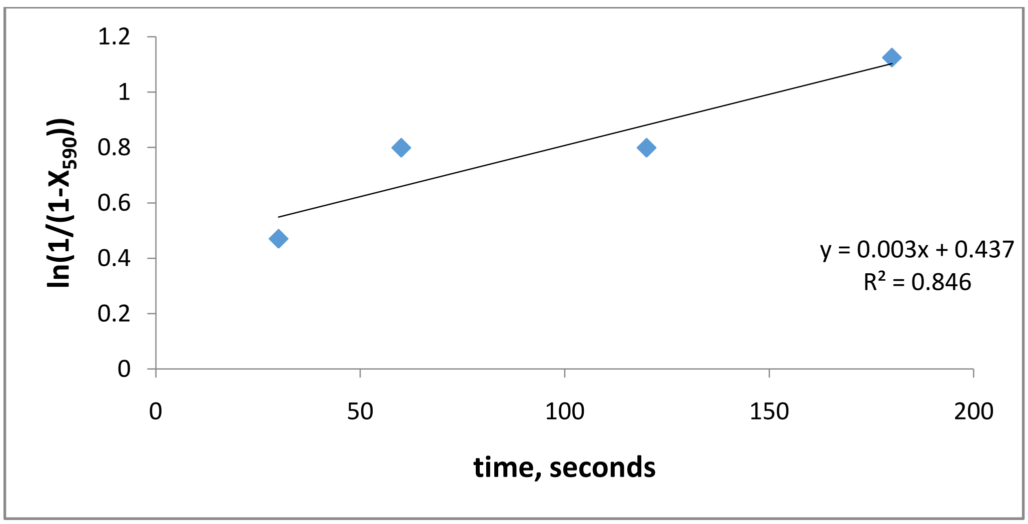

Figure 4.13: Testing first order model for commercial zeolite Y at 590˚C

From Figures 4.14 to 4.17 it can be seen that the second order describes the kinetics of catalytic cracking using the commercial zeolite better than the first order plots, as this was later confirmed by the Arrhenius plots having a better correlation.

The second order kinetics was an indication of both acid sites contributing greatly to the catalytic cracking of the heavy gas oil and hence indicate the easy formation of the Lewis sites at higher temperature.

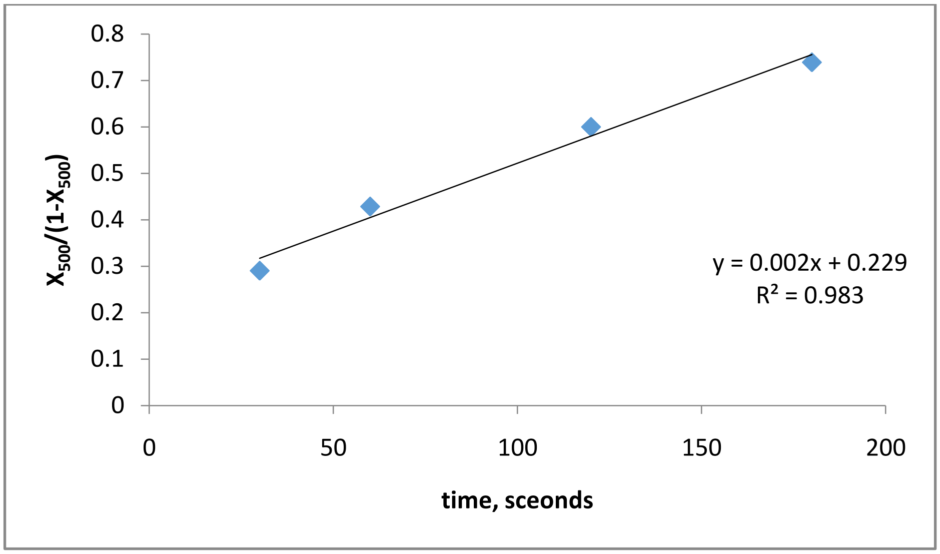

Figure 4.14: Testing second order model for commercial zeolite Y at 500˚C

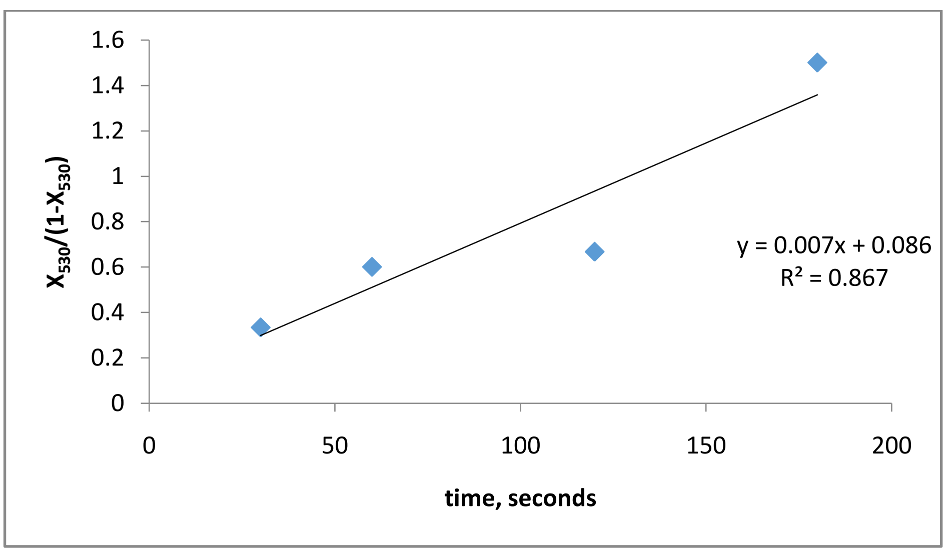

Figure 4.15: Testing second order model for commercial zeolite Y at 530˚C

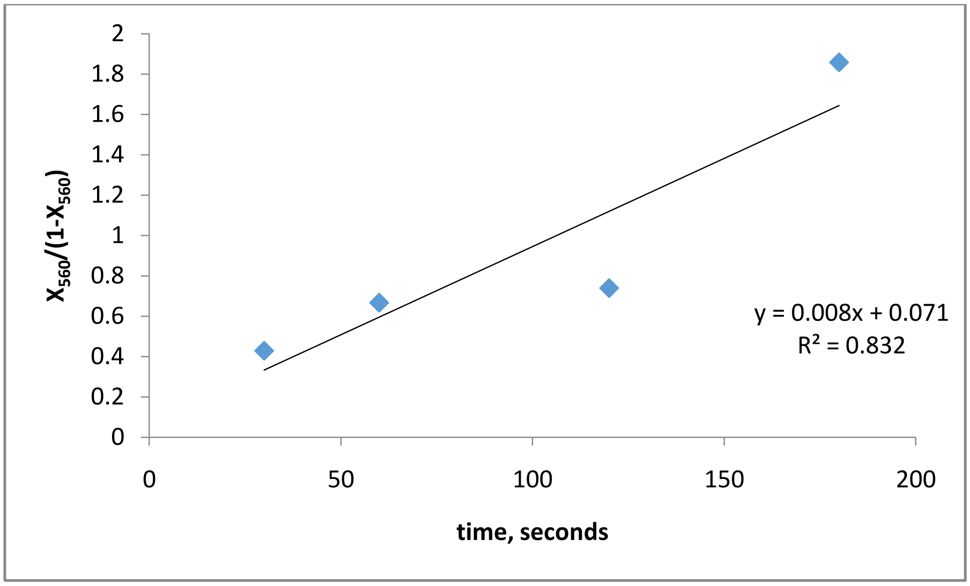

Figure 4.16: Testing second order model for commercial zeolite Y at 560˚C

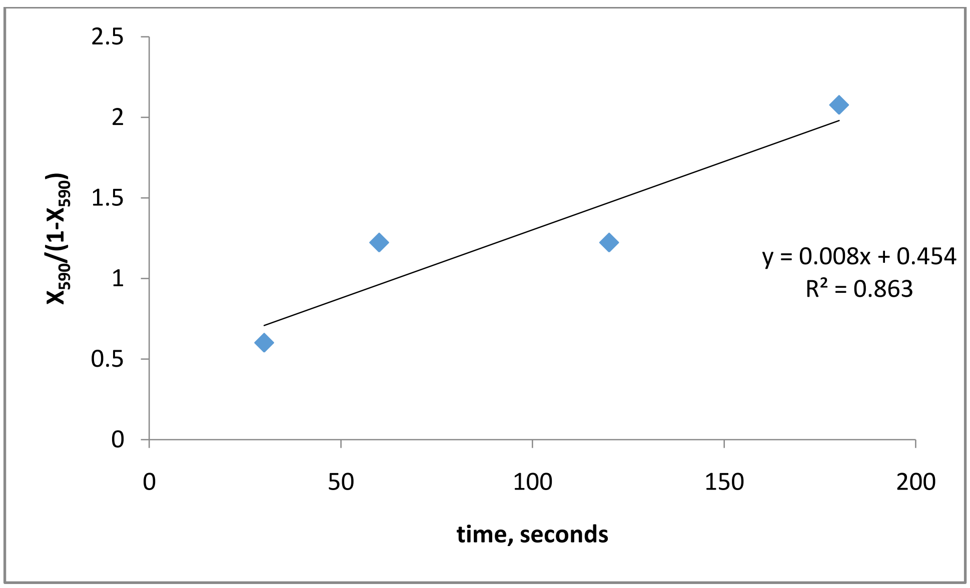

Figure 4.17: Testing second order model for commercial zeolite Y at 590˚C

4.3.3 Catalytic cracking using zeolite Y/ZSM-5

The kinetics describing the catalytic cracking of heavy gas oil using the composite zeolite Y/ZSM-5 was found to be second order as shown in Figures 4.18 to 4.21, and this change of reaction order was expected as a result of addition of ZSM-5 to zeolite Y. This change from a unimolecular reaction to a bimolecular reaction could be attributed to the contribution of both the Bronsted acid sites and the Lewis acid sites in the catalytic cracking reaction of the heavy gas oil.

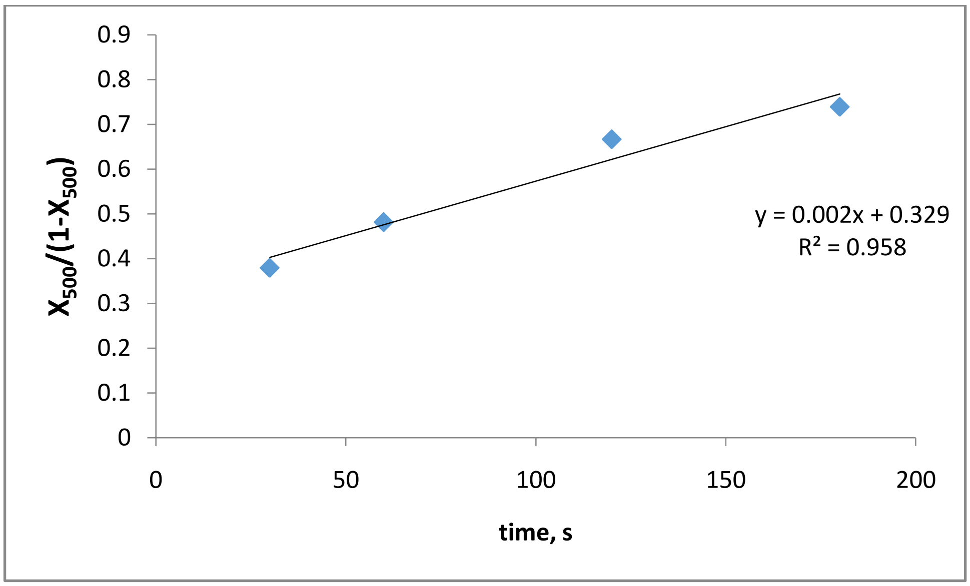

Figure 4.18: Second order model for zeolite Y/ZSM-5 at 500˚C

The poor correlation coefficient at 560˚C with 61.79% indicated the deviation from second order kinetics which confirms with the report by Farouq T. *et al.*, (2004) that the feedstocks of petroleum hydrocarbons showed variable order in the range of 1.6-1.9.

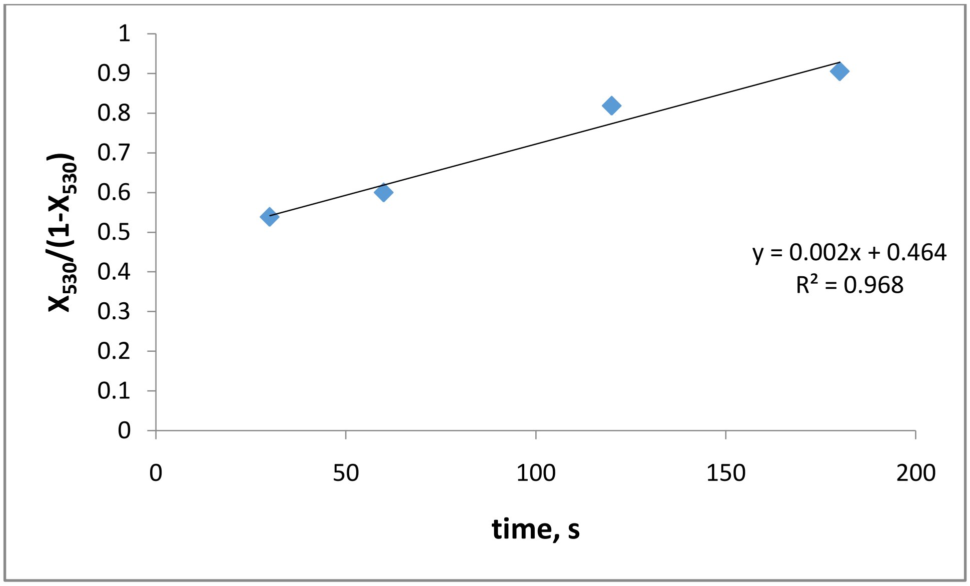

Figure 4.19: Second order model for zeolite Y/ZSM-5 at 530˚C

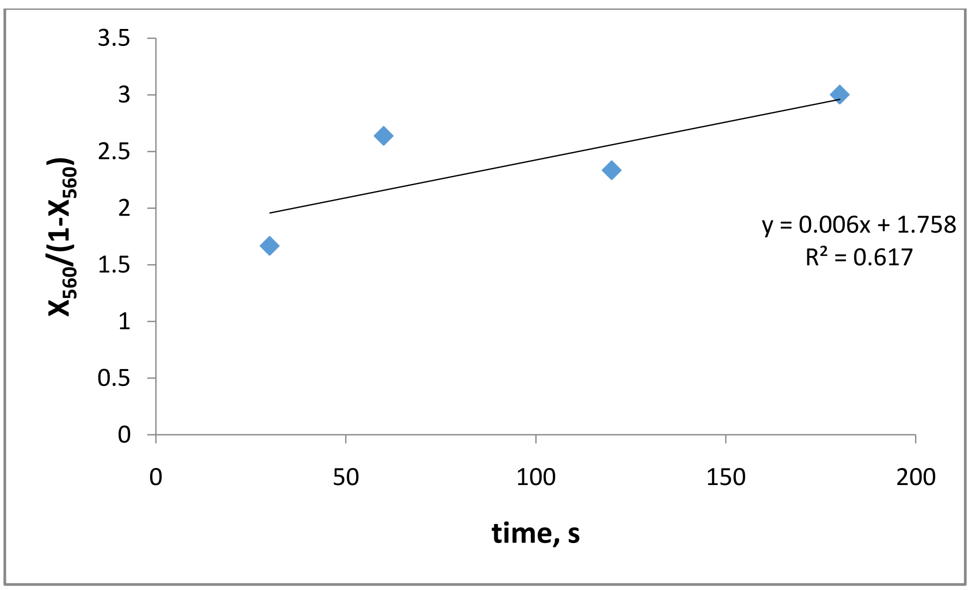

Figure 4.20: Second order model for zeolite Y/ZSM-5 at 560˚C

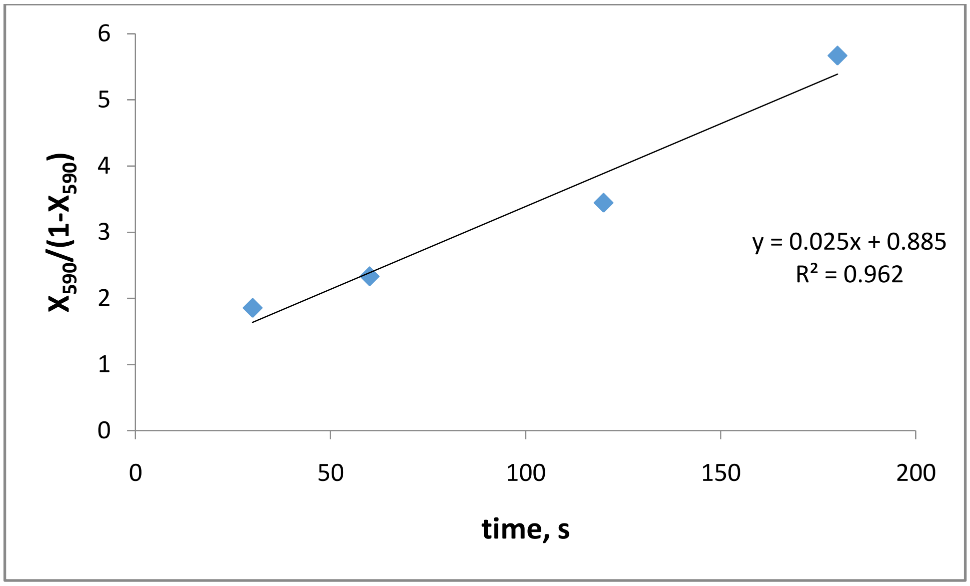

Figure 4.21: Second order model for zeolite Y/ZSM-5 at 590˚C

4.4 Comparison of Kinetic Parameters

It can beobserved from Table 4.6, that the values of rate constants for the kinetics using the commercial zeolite Y were greater than those for synthesized zeolite Y. This may mean thatthe commercial zeolite Yhad higher acid site density than the synthesized zeolite Y. The higher activity may also be attributed to some water molecules occluded in the commercial zeolite Y structure which increases the formation of more hydroxonium ions and hence more Bronsted acid sites(Aderemi *et al*., 2001).

It was also observed from Table 4.6 that there was a decrease in the value of k_{comY2} from 560˚C to 590˚C; this is due to the reduced activity of the catalyst as a result of complete loss of hydroxonium ions responsible for the Bronsted site in the commercial zeolite Y (Aderemi *et al*., 2001).

Table 4.6: Values of rate constant for catalytic cracking of HGO using synthetized and commercial zeolite Y

Temperature, ˚C	k_{synY}, s^{-1}	R^2_{synY}	k_{comY2}	R^2_{comY2}
500	0.0021	0.9525	0.0029	0.9831
530	0.0023	0.9731	0.0071	0.8677
560	0.0032	0.9954	0.0087	0.8320
590	0.0040	0.9940	0.0085	0.8636

Table 4.6 further showed that between 500˚C to 530˚C, a percentage increase of 9.52% in the value of k_{synY} is observed while between 530˚C to 560˚C we have 39.13%, this sharp increase may be attributed to formation of more Lewis site for catalytic cracking and also formation of free radicals at elevated temperature, since thermal cracking is favored at higher temperature (Bruce *et al*. 1979). For the commercial zeolite this sharp increase is observed between 500˚C and 530˚C could be due to formation of Lewis site which contributes greatly to the cracking of the heavy gas oil.

Table 4.7 showed the rate constants for the cracking reaction using synthesized zeolite Y/ZSM-5 and it can be observed that addition of ZSM-5 increased the rate of reaction (indicated by the increase in rate constants) at each operating condition of temperature and this can be attributed to the shape-selective mechanism of ZSM-5 as it cracks hydrocarbon molecules that pass through the pores of zeolite Y without being cracked (Mustapha *et al*., 2006), thus reduces the diffusional constraints of the molecules through the zeolite Y matrix, thus increasing the rate of catalytic cracking.

Table 4.7: Rate constant value for synthesized zeolite Y/ZSM-5

T, K	$k_{Y/ZSM-5}$	1/T, K^{-1}	$\ln k_{Y/ZSM-5}$
773	0.0024	0.0013	-6.0322
803	0.0026	0.0012	-5.9522
833	0.0067	0.0012	-5.0056
863	0.0250	0.0011	-3.6888

Between temperatures of 560˚C and 590˚C in Table 4.7, it could be deduced that there was a very high increase of about 273.13% in the rate constants from 560˚C to 590˚C; this may be due to contribution of more Bronsted acid sites from zeolite ZSM-5 added to the synthesized zeolite Y and at highertemperatures the kerosene and diesel fractions are also undergoing secondary reactions into other products such as light gases, gasoline fractions and molecules even higher than the diesel range.

To show that the experimental data obeyed the Arrhenius equation, a graph of ln(k) versus 1/T (K^{-1}) was plotted and a linear relationship with a negative slope existed for both synthesized zeolite Y, commercial zeolite Y and zeolite Y/ZSM-5 as shown in Figures 4.22 to 4.25 except for the Arrhenius plot for the first order kinetics using the commercial zeolite Y in Figure 4.23 having a very low correlation coefficient and also seemed to be more non-linear than a linear graph.

From Figures 4.22 to 4.25, the activation energy, E_a of the catalyst can be evaluated from the Arrhenius equation where the slope of the graph equals ratio of activation energy to molar gas constant and the intercept is equal to the pre-exponential factor. The Arrhenius equation is shown in Equation 4.1

$$k = A_0 exp\left(-\frac{E_a}{R.T}\right) \qquad \ldots(4.1)$$

$$lnk = lnA_0 - \frac{E_a}{R.T} \qquad \ldots(4.2)$$

Where R is the molar gas constant, $R = 8.314 J/(mol.K)$

A_0 is the pre-exponential factor

E_a is the activation energy, J/mol

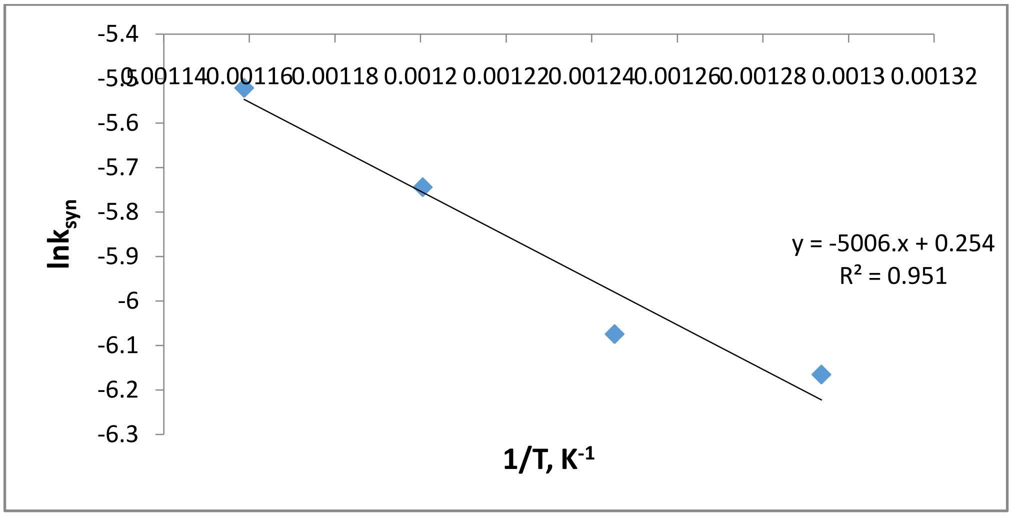

Figure 4.22: Linearity of experimental data for synthesized zeolite Y, first order kinetics

From Figure 4.22, it can be concluded from the Arrhenius plot that the catalytic cracking reaction of heavy gas oil using the synthesized zeolite Y can be described by the first order kinetics since it gave us a linear plot and a good correlation coefficient of 95.16%; Farouq *et al*. (2004) reported that most of the cracking reaction of pure hydrocarbons followed first order kinetics.

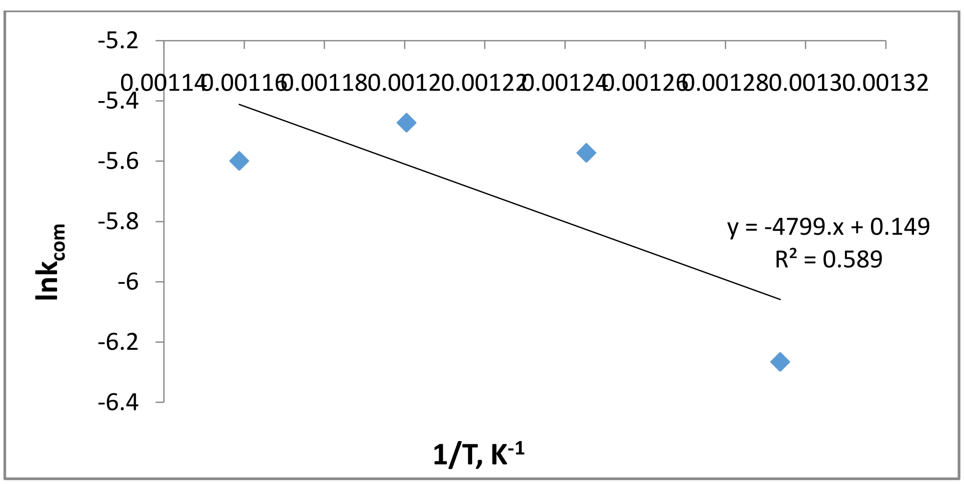

Figure 4.23: Linearity of experimental data for commercial zeolite Y, first order kinetics

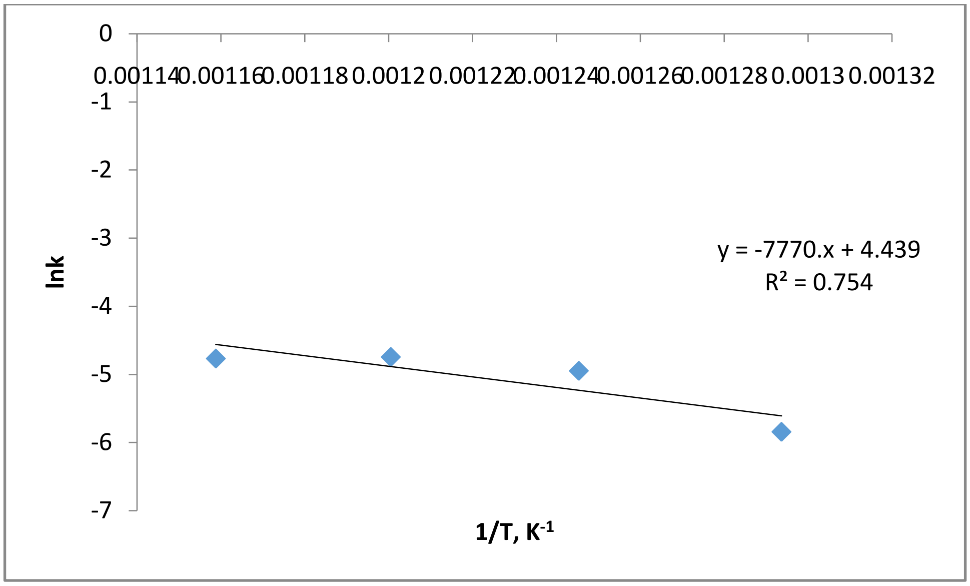

Figure 4.24: Linearity of experimental data for commercial zeolite, second order kinetics

Comparing Figures 4.23 with 4.24, it was shown that the second order kinetics best described the catalytic cracking of the heavy gas oil using the commercial zeolite Y, Farouq *et al*., (2004) reported that the cracking reaction of the feedstocks of petroleum hydrocarbons showed a variable order in the range of 1.6 to 1.9, Al-Khattaf, (2003) also reported that the activity of FCC catalyst is evaluated based on the second order conversion.

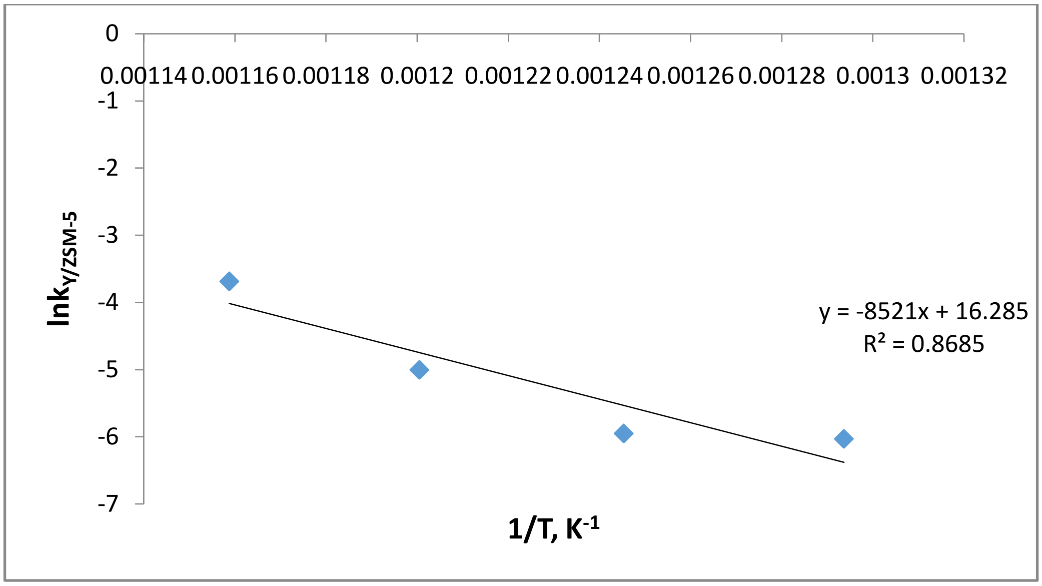

Figure 4.25: Linearity of experimental data for zeolite Y/ZSM-5

Figure 4.25 showed a very high correlation coefficient indicating that the kinetics of catalytic cracking reaction using the zeolite Y/ZSM-5 catalyst can be described by second order kinetic model. The activation energies of these reactions are summarized in Table 4.8.

The values of the activation energy and the pre-exponential factors for the three catalysts were evaluated from the slope and intercept of Figures 4.22 to 4.25 and results tabulated in Table 4.8.

Table 4.8: Activation energy and pre-exponential factor of each catalyst

	E_a, kJ/mol	A_0
Synthesized zeolite Y, 1st order	41.6249	1.2894
Commercial zeolite Y, 2nd order	64.6006	4.4392
Zeolite Y/ZSM-5, 2nd order	70.8436	16.285

The activation energies for the three catalysts as shown in Table 4.8 indicated that catalytic cracking mechanism predominates within the reaction conditions as the average activation energy of hydrocarbon cracking is in the order of 41.8 – 62.76kJ/mol while the activation energy for thermal cracking is about 229.9kJ/mol (Daniel, 1984).

The significance of the pre-exponential factor indicates the number of collisions of hydrocarbon molecules in the heavy gas oil and also number of adsorbed molecule on the catalyst per second that result into a product. From Table 4.8, it can also be observed that the pre-exponential factor for the zeolite Y/ZSM-5 is highest; it indicated the number of favorable collisions and then cracking that resulted into product, this also confirmed the initial assumption of the reduction in the diffusional constraints of heavier molecules through zeolite Y catalyst. The commercial zeolite Y has a pre-exponential factor of 4.4392; it also showed a better effective collision of hydrocarbon molecules with the catalyst site than the synthesized zeolite Y.

4.5 Effect of Reaction Time on Conversion of Heavy Gas Oil

Figures 4.26, 4.27 and 4.28 showed the effect of time on HGO conversion for synthesized zeolite Y, commercial zeolite Y and synthesized zeolite Y/ZSM-5 respectively. As shown in these figures, the HGO conversion increases with increase in time. This might possibly be due to more of the heavy gas oil heated and more vapors are produce at constant temperature and also more time is available for the carrier gas to take more of the oil vapor in contact with the catalyst.

Figure 4.26 showed an approximately linear relationship between conversion and time which confirms the first order kinetics as shown in the first order plots for the synthesizedzeolite Y, this linearity was not observed in the case of the commercial zeolite Y and the synthesized zeolite Y/ZSM-5 at 560˚C this was as a result of the deviation from first order kinetics, the second order kinetics therefore describes better the experimental data for commercial zeolite Y and synthesized zeolite Y/ZSM-5.

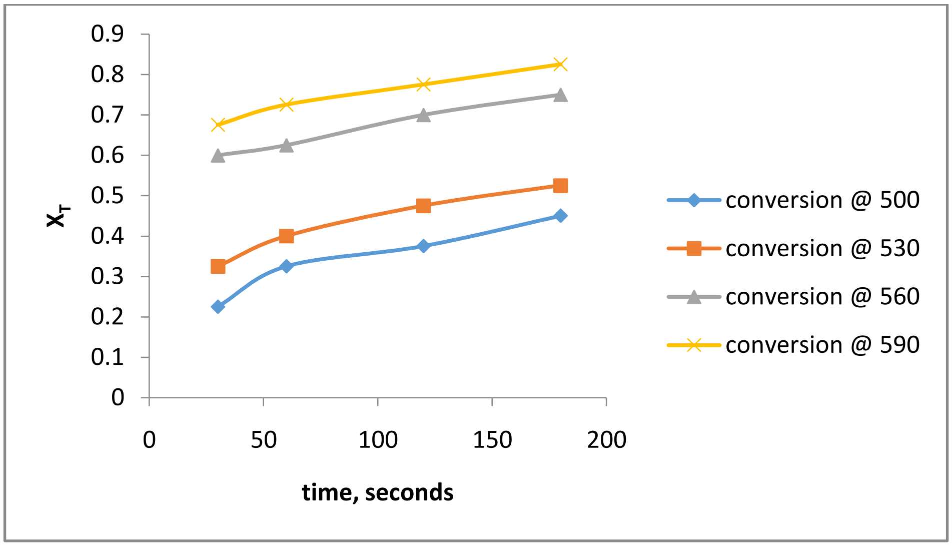

Figure 4.26: Effect of time on conversion using synthesized zeolite Y

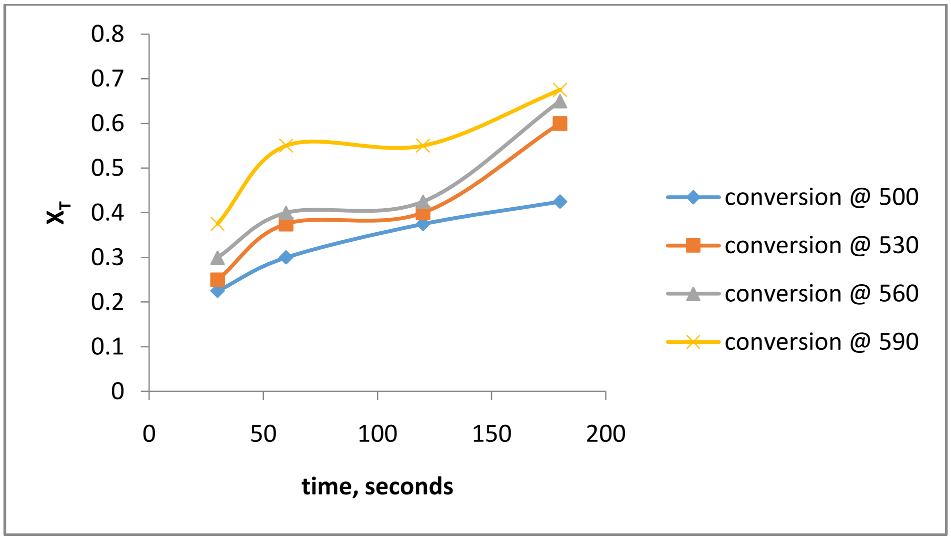

Figure 4.27: Effect of time on conversion using commercial zeolite Y

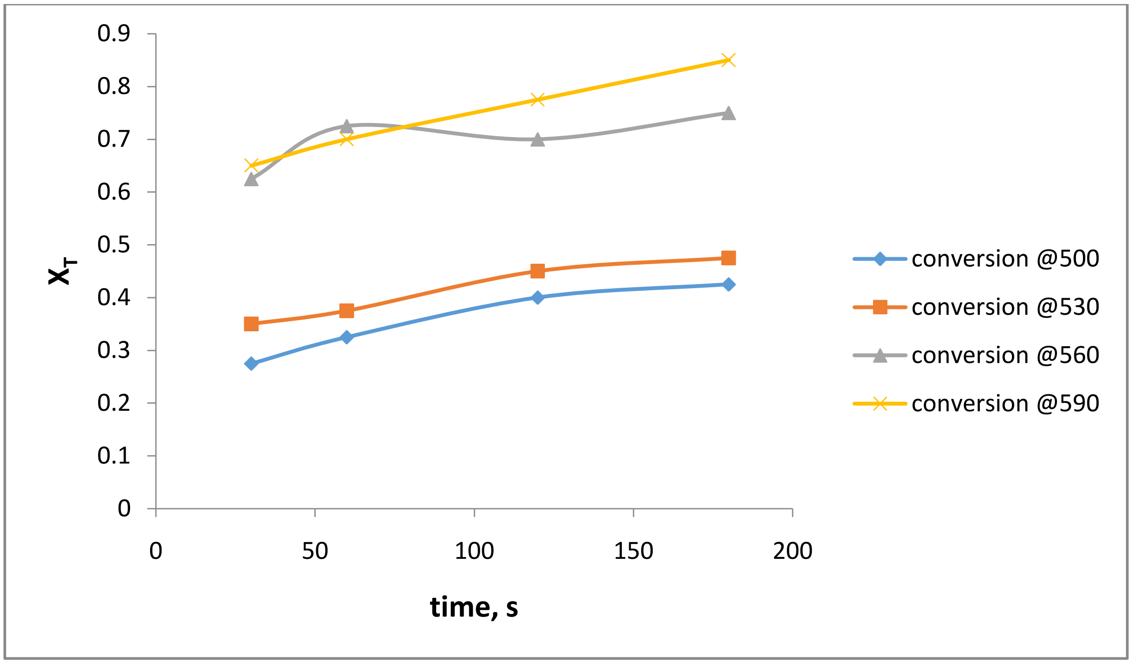

Figure 4.28: Effect of time on conversion using zeolite Y/ZSM-5

4.6 Effect of Temperature on Conversion of Heavy Gas Oil

Figures 4.29, 4.30 and 4.31 showthe effect of temperature on HGO conversion over synthesized zeolite Y, commercial zeolite Y and zeolite Y/ZSM-5 respectively. As shown in these figures, the HGO conversion increases with increase in temperature. This might possibly be due to increasing intermolecular motions, which assists the transformations of the reactants into new compounds and thus enhances the rate of chemical reaction. Generally, catalytic cracking reaction is thermodynamically favored at high temperature (Bruce *et al*. 1979) which explains the increase in conversion with temperature. The higher temperature provided advantages in terms of a better feed vaporization. Also increased temperature enhances the overall conversion of the heavy gas oil by enhancing the rates of protolysis of paraffins and decomposition reactions as α- and β-scission (AdulHalim *et al.*, 2010).

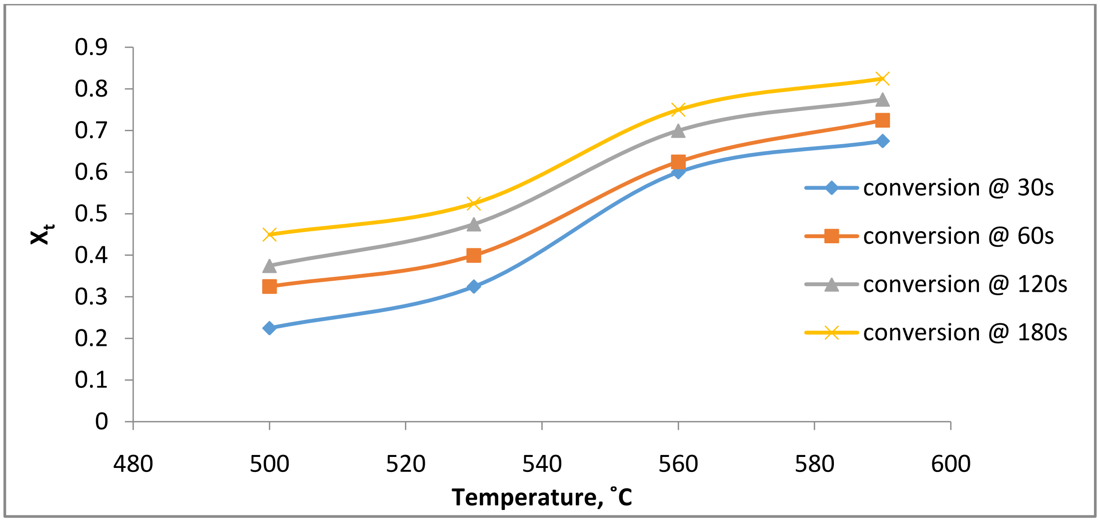

Figure 4.29: Effect of temperature on conversion for synthesized zeolite Y

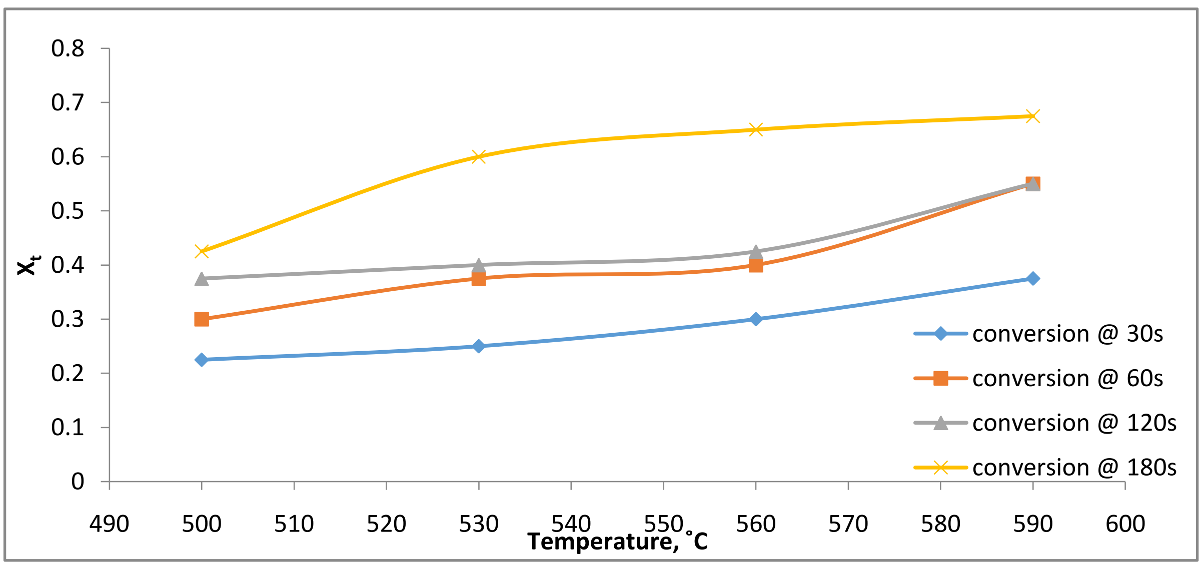

Figure 4.30: Effect of temperature on conversion for commercial zeolite Y

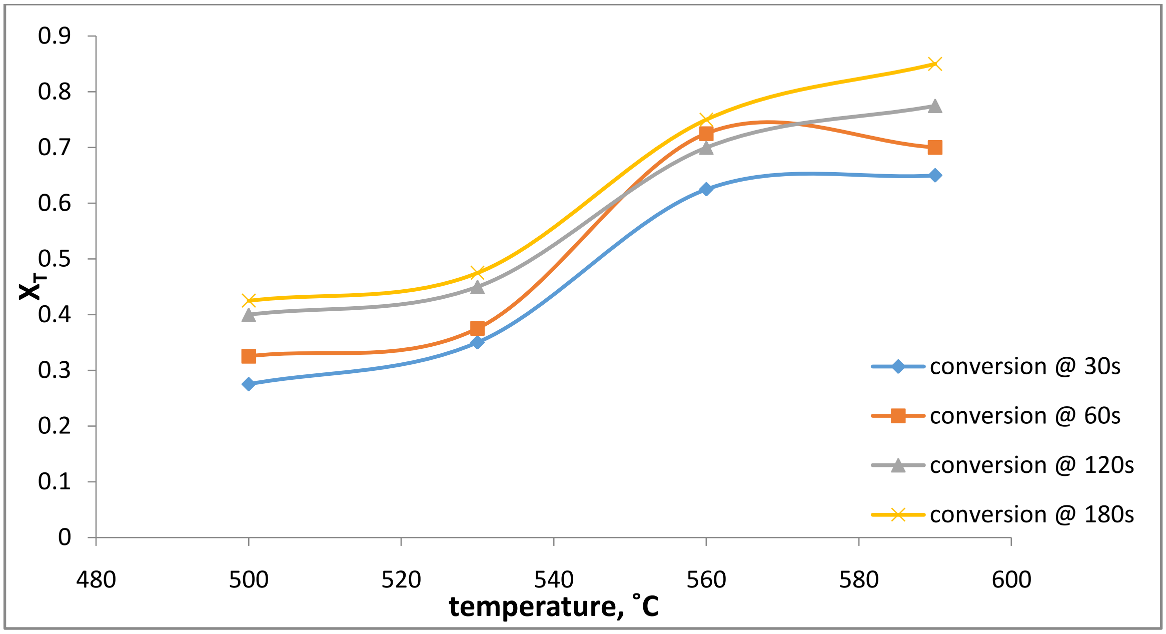

Figure 4.31: Effect of temperature on conversion for zeolite Y/ZSM-5

The differences in the conversion among the three catalysts also indicate that heavy gas oil conversion is a strong function of the crystallite size, as the amount of gas oil converted depends on the pore diffusion resistance within the crystallite network (Mustafa *et al.*, 2006). We can therefore suggest that zeolite Y/ZSM-5 with the highest conversion (85% at 590˚C) has a larger pore size than the synthesized zeolite Y (82.5% at 590˚C) and commercial zeolite Y (67.5% at 590˚C) with the lowest pore size, calculation on conversion of the heavy gas oil is presented in appendix B.

4.7 Effect of Temperature on the Yield of Kerosene and Diesel Fractions

It was observed in Figures 4.32 to 4.35 that at 500˚C and 530˚C, the yield of kerosene and diesel fractions tend to decrease with increase in time, this phenomenon can be attributed to the conversion of heavier fractions in the kerosene and diesel range to other lighter fractions, this is due to more Bronsted acid sites at these conditions which is responsible for cracking the molecules to fractions lighter than the kerosene and diesel range.

It was also observed in Figures 4.32 to 4.35, that the yield of kerosene and diesel tend to increase with increase in time at 560˚C and 590˚C, this trend can be attributed to the formation of Lewis acid sites at higher temperature, this Lewis acid sites are weaker acid sites, so the heavy gas molecules will not be over-cracked hence, more of the kerosene and diesel fractions will be observed at higher temperature.

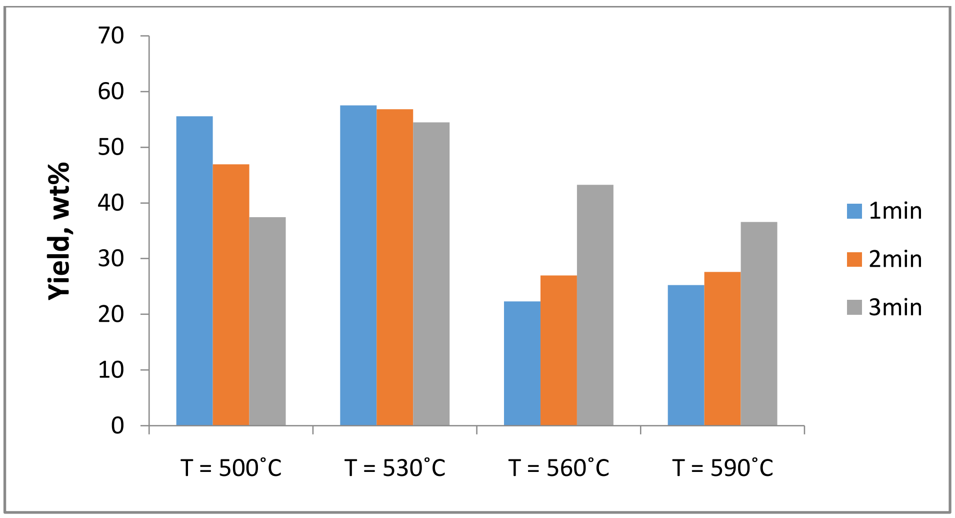

Figure 4.32: Effect of time on yield of kerosene using synthesized zeolite Y

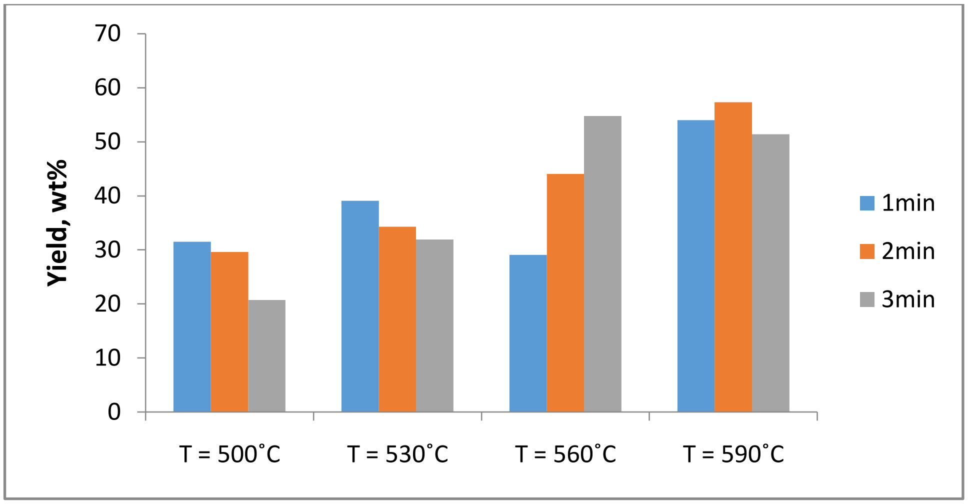

Figure 4.33: Effect of time on yield of diesel using synthesized zeolite Y

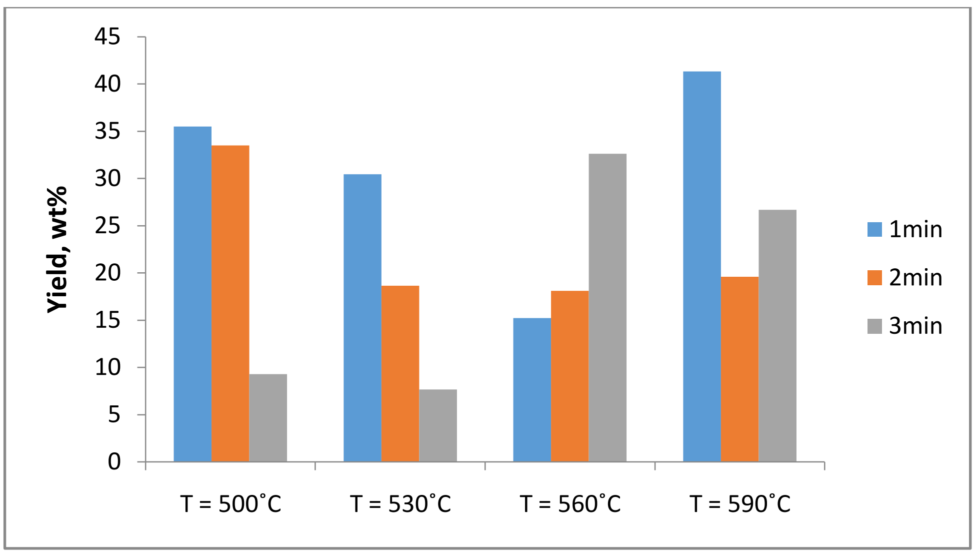

Figure 4.34: Effect of time on yield of kerosene using commercial zeolite Y

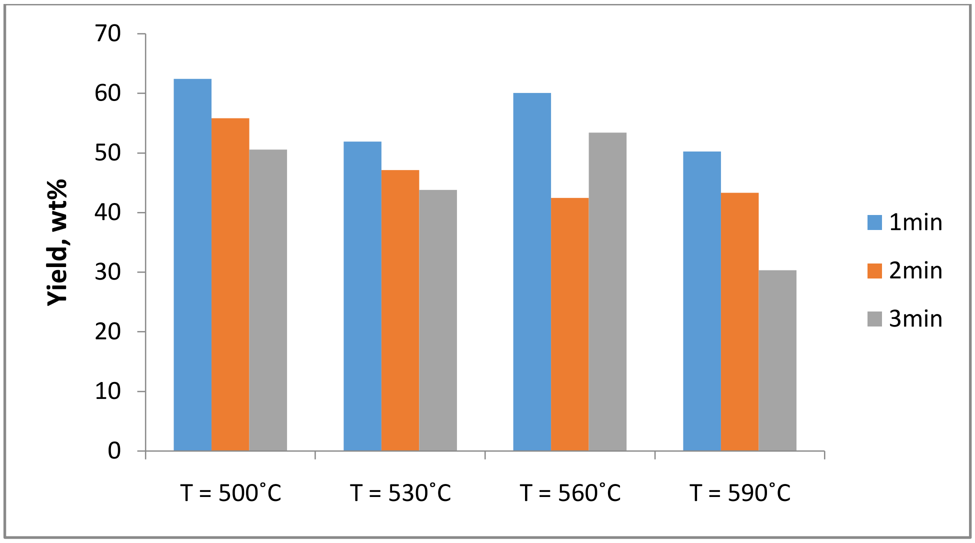

Figure 4.35: Effect of time on yield of diesel using commercial zeolite Y

4.8 Effect of Blending ZSM-5 Zeolite in Zeolite Y

It could be observed from Figure 4.36 that the yield of kerosene and diesel from both the synthesized and commercial zeolite Y are higher than the yield of kerosene and diesel when compared with the blended zeolite, synthesized zeolite Y/ZSM-5. This reduction can be due to the fact that zeolite ZSM-5 incorporated in the blend can crack fractions of the kerosene and diesel range into lighter fractions such as gasoline and lighter gases. This effect of the ZSM-5 zeolite in the blend is reflected in the higher yield of the gasoline fraction, and a corresponding reduction in the yield of kerosene and diesel fractions.

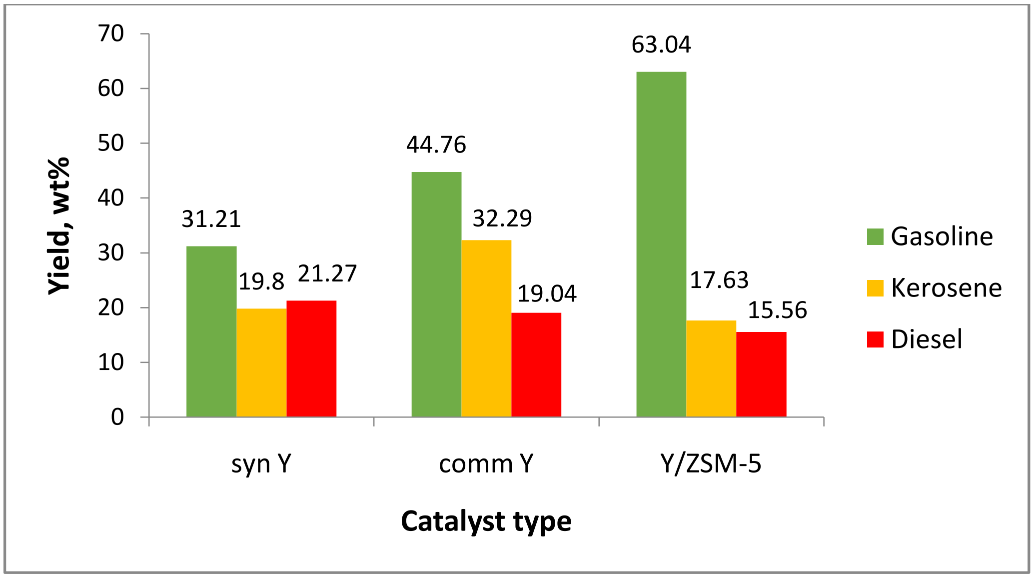

Figure 4.36: Comparative yield of fractions using synthesized zeolite Y, commercial zeolite Y and zeolite Y/ZSM-5 at 500˚C, 1 minute.

CHAPTER FIVE

CONCLUSIONS AND RECOMMENDATIONS

5.1 CONCLUSIONS

1. The experimental results indicated that catalytic reaction predominated over thermal cracking as seen from the values of activation energy of 41.624kJ/mol, 64.6006kJ/mol and 70.8436kJ/mol for the synthesized zeolite Y, commercial zeolite Y and synthesized zeolite Y/ZSM-5 respectively.
2. The results also showed that catalytic cracking using synthetic zeolite Y was better described by first order kinetics while using commercial zeolite Y and the synthesized zeolite Y/ZSM-5 were better described by second order kinetics.
3. Using the synthesized and commercial zeolite Y, the yield of kerosene and diesel fractions both decreased with increase in time at 500˚C and 530˚C, but at 560˚C and 590˚C the yield of kerosene and diesel fractions increased with time.
4. The effect of adding zeolite ZSM-5 in zeolite Y indicated a significant contribution in the catalytic cracking process as 63.04% yield of gasoline was observed at 560˚C for 1minutecompared to 31.21% gasoline yield at 530˚C for 1minute using the synthesized zeolite Y while the maximum yield of gasoline using the commercial zeolite Y was 44.76% at 560˚C for 1min.

5.2 RECOMMENDATIONS

1. Further work should be done by changing the size of silica-glass tube in order to vary the weight of the catalyst so that the effect of catalyst weight on the product of the fractions can be studied.

2. Further work should also be carried out by varying pressure of the nitrogen gas (carrier gas) as this parameter affects the adsorption of molecules on the surface of the catalyst.

3. Provision of online gas chromatograph.

fREFERENCES

Abdel-Aal, H. K., Bakr, B. A., Al-Sahlawi, M. and Marcel D. (1992). *Petroleum Economics and Engineering*, Inc., p 309.

AbdulHalim, A. K. M. and Karim, K. E. (2010). Fluid Catalytic Cracking of Petroleum Fraction (Vacuum Gas Oil) to Produce Gasoline. *Iraqi Journal of Chemical and Petroleum Engineering, Vol.11 No.4*p 33-45

AbdulHalim, A. K.M.; Rawa, G. Y. andKarim, K. E. (2011). Cracking Activity of Prepared Y-Zeolite Catalyst Using Cumene on Fluidized Bed Reactor. *Iraqi Journal of Chemical and Petroleum Engineering, Vol.12 No.2* p9-7

Aderemi. B. O., Oludipe, J. O. and Adefila, S. S. (2001). Evaluation of Catalytic Cracking Potential of a Locally Synthesized zeolite-A: Comparative Study, *Nigeria Journal of Engineering, Vol. 9*, p 66-74.

Affum, H. A., Mumuni, I. I., Appiah, G. K., Adzaklo, S. Y. and Addo, M. A. (2013). On The Conversion of Gas Oil in Fluid Catalytic Cracking Risers: Application of Residence Time Distribution Concept, *International Journal of Scientific and Technology Research, Vol. 2*, p 168-173.

Ahmed M. A. A. (2007). Development of Niw-Zeolite-Based Catalysts for Hydrocracking of Gas Oil: Synthesis, Characterization, Activity and Kinetic Studies, Unpublished Ph.D Thesis, Department of Chemical Engineering, University Sains Malaysia.

Al-khataf, S. (2003). The Influence of Alumina on the Performance of FCC Catalysts during Hydrotreated VGO Catalytic Cracking, *Journal of Energy and Fuels, Vol. 17*, p 62-68.

Bruce, C. G; James, R. K. and Schuit, G. C. A. (1979). *Chemistry of Catalytic Processes*, McGraw-Hill, New York.

Chaohe, Y., Zheng, H., Du, F. and Xu, C. (1997). Reaction Characteristics and Mechanism of Residuum Hydrocracking, University of Petroleum, China.

Daniel Decrooq, (1984). *Catalytic Cracking of Heavy Petroleum Fractions*. 1st Edition, Technip, Paris.

Den-Hollander, M. A; Wissink, M; Makkee, M. and Moulijn, J. A. (2002). Gasoline Conversion: Reactivity towards Cracking with Equilibrated FCC and ZSM-5 Catalysts. *Journal of Applied Catalysis, Vol. 223* p 85–102

Erikh, V. N., Rasina, M. G. and Rudin, M. G. (1988). *The Chemistry and Technology of Petroleum and Gas*. Mir Publishers, Moscow. p 39-134.

Farouq, T., AbdulRahman, M. and Subhash, B. (2004). Catalytic Cracking of Palm Oil into Liquid Fuels: Kinetic Study, The Seventh Asia-Pacific International Symposium on Combustion and Energy Utilization.

Harold, A. W., Bryan, G. R. and Jeffrey, S. P. (2004). *Industrial Organic Chemicals*, (2nd Edition), John Wiley and Sons.

Jacob, S. H., Gross, B., Voltz, S. E. and Weekman V. M. (1976). A Lumping and Reaction Scheme for Catalytic Cracking. *Journal of AIChE, Vol. 22*, p 701-713.

John, D. and David, J. R. (1993). Fluid Catalytic Cracking: Chemistry, *Catalysis Today, Vol. 18*, p 487-507.

Juarez, A. J., Lopez, I. F. and Aguilar, R. E. (1999). 5-Lump Kinetic Model for Gas Oil Catalytic Cracking, *Journal of Applied Catalysis, Vol. 177*, p 227-235.

Mustapha, A.; Jesus, A. A. and Hugo, L. (2006). Kinetic Modeling of Catalytic Cracking of Gas oil Feedstocks: Reaction and Diffusion Phenomena, *Journal of Industrial Engineering and Chemical Research, Vol. 45*, p 1583-1593.

Niken, T., Abdulrahman, M. and Subhash, B. (2011). Nano-crystalline Zeolite Y: Synthesis and Characterization, *Journal of Material Science and Engineering*, IOP publishing.

Rajkumar, G. S. (2005). *Modeling and Simulation of Fluid Catalytic Cracking Unit*, (Doctoral dissertation,Submitted to the Department of Chemical Engineering Thepar Institute of Engineering and Technology, Patiala, India).

Ronald, W. M; Charles, A. M. and Bradley, A. S. (1999). *Introduction to Chemical Reaction Engineering and Kinetics*, John Wiley and Sons, New York.

Sadeghbeighi, R. (1995). *Fluid Catalytic Cracking Handbook*, (2nd Edition), Butterworth-Heinemann.

Scott, J. W. and Bridge, A. G.(1971). Origin and Refining of Petroleum, *American Chemical Society, No. 7*p 116.

Speight, J. G. (2006). *The Chemistry and Technology of Petroleum*. CRC Press.

Speight, J. G. (2007). *The Chemistry and Technology of Petroleum*, (4th Edition) edition. CRC Press.

Weekman, V.W., and Nace, D. M. (1970). Kinetics of Catalytic Cracking Selectivity in Fixed, Moving and Fluid-bed Reactors, *Journal of AIChE, Vol. 16*, p397-404.

Yen, L., Wrench, R. and Ong, A. (1987). Reaction Kinetic Correlation for Predicting Coke Yield in Fluid Catalytic Cracking. *Presented at the Katalistisks 8th Annual Fluid Catalytic Cracking Symposium, Budapest, Hungary*.

APPENDICES

APPENDIX A: Calibration of tube furnace and Calibration of standards using gas chromatograph

Appendix A shows the calibration reading of the catalytic cracking units and also the calibration of the gas chromatograph used.

Table A1: Calibration result for the tube furnace

Percentage reading, %	Actual temperature, ˚C	Furnace reading, ˚C
10	220	140
20	380	240
30	490	330
40	590	400
50	670	490
60	800	580
80	1020	760

The concentrations of the individual components are evaluated from the equation of line of the GC calibration graph in the main work.

Calibration of standards on samples from synthesized zeolite Y

Table A2: Concentration of components in the cracked product at 500˚C, 1minutes using synthesized zeolite Y

C_{HGO}	Component	C_P, mg/ml	W_{HGO}, mg	W_P, mg
0.038	C10	0.0381	0.494	0.4953
0.3445	C10=	0.3539	4.4785	4.6007
0.1175	C12	0.075	1.5275	0.975
0.4938	C12=	0.8883	6.4194	11.5479
0.4211	C14	4.4594	5.4743	57.9722
5.3258	C14=	8.0176	69.2354	104.2288
1.0715	C16	1.7227	13.9295	22.3951
8.2115	C16=	3.0753	106.7495	39.9789
2.7291	C20	1.3786	35.4783	17.9218
8.4796	C22	5.8298	110.2348	75.7874
0	C24	1.8923	0	24.5999
3.847	C28	0.6984	50.011	9.0792

Table A3: Concentration of components in the cracked product at 500˚C, 2minute using synthesized zeolite Y

Component	C_P, mg/ml	W_{HGO}, mg	W_P, mg
C10	0.0395	0.57	0.5925
C10=	0	5.1675	0
C12	0.2847	1.7625	4.2705
C12=	0.7857	7.407	11.7855
C14	0	6.3165	0
C14=	0	79.887	0
C16	8.9036	16.0725	133.554
C16=	5.6839	123.1725	85.2585
C20	2.5578	40.9365	38.367
C22	4.5049	127.194	67.5735
C24	0.9276	0	13.914
C28	1.2136	57.705	18.204

Table A4: ***Concentration of components in the cracked product at 500˚C, 3minutes using synthesized zeolite Y***

Component	C_P, mg/ml	W_{HGO}, mg	W_P, mg
C10	0.0589	0.684	1.0602
C10=	0.3647	6.201	6.5646
C12	0.3301	2.115	5.9418
C12=	1.1147	8.8884	20.0646
C14	0	7.5798	0
C14=	0	95.8644	0
C16	8.36	19.287	150.48
C16=	3.2772	147.807	58.9896
C20	1.2869	49.1238	23.1642
C22	2.6868	152.6328	48.3624
C24	2.0195	0	36.351
C28	0.4474	69.246	8.0532

Table A5: ***Concentration of components in the cracked product at 530˚C, 1minute using synthesized zeolite Y***

C_{HGO}	Component	C_P, mg/ml	W_{HGO}, mg	W_P, mg
0.038	C10	0	0.608	0
0.3445	C10=	0	5.512	0
0.1175	C12	0.4034	1.88	6.4544
0.4938	C12=	1.9936	7.9008	31.8976
0.4211	C14	6.6472	6.7376	106.3552
5.3258	C14=	0.9483	85.2128	15.1728
1.0715	C16	3.9232	17.144	62.7712
8.2115	C16=	6.3654	131.384	101.8464
2.7291	C20	0	43.6656	0
8.4796	C22	6.3577	135.6736	101.7232
0	C24	4.447	0	71.152
3.847	C28	1.3399	61.552	21.4384

Table A6: ***Concentration of components in the cracked product at 530˚C, 2minutes using synthesized zeolite Y***

C_{HGO}	Component	C_P, mg/ml	W_{HGO}, mg
C10	0.0392	0.722	0.7448
C10=	0.3561	6.5455	6.7659
C12	0.4088	2.2325	7.7672
C12=	0.8532	9.3822	16.2108
C14	0	8.0009	0
C14=	0.8715	101.1902	16.5585
C16	10.4427	20.3585	198.4113
C16=	6.356	156.0185	120.764
C20	0	51.8529	0
C22	8.0703	161.1124	153.3357
C24	1.5029	0	28.5551
C28	1.0893	73.093	20.6967

Table A7: ***Concentration of components in the cracked product at 530˚C, 3minutes using synthesized zeolite Y***

C_{HGO}	Component	C_P, mg/ml	W_{HGO}, mg
C10	0.0539	0.798	1.1319
C10=	0.3506	7.2345	7.3626
C12	0.3297	2.4675	6.9237
C12=	0.6123	10.3698	12.8583
C14	2.2158	8.8431	46.5318
C14=	3.7719	111.8418	79.2099
C16	7.0212	22.5015	147.4452
C16=	3.9175	172.4415	82.2675
C20	0	57.3111	0
C22	0	178.0716	0
C24	1.4333	0	30.0993
C28	8.4821	80.787	178.1241

Table A8: ***Concentration of components in the cracked product at 560˚C, 1minute using synthesized zeolite Y***

C_{HGO}	Component	C_P, mg/ml	W_{HGO}, mg	W_P, mg
0.038	C10	0.0545	0.95	1.3625
0.3445	C10=	0	8.6125	0
0.1175	C12	0.3688	2.9375	9.22
0.4938	C12=	0	12.345	0
0.4211	C14	0.1675	10.5275	4.1875
5.3258	C14=	0.5214	133.145	13.035
1.0715	C16	2.8965	26.7875	72.4125
8.2115	C16=	3.3481	205.2875	83.7025
2.7291	C20	3.9361	68.2275	98.4025
8.4796	C22	1.7099	211.99	42.7475
0	C24	2.0746	0	51.865
3.847	C28	1.3505	96.175	33.7625

Table A9: ***Concentration of components in the cracked product at 560˚C, 2minutes using synthesized zeolite Y***

Component	C_P, mg/ml	W_{HGO}, mg	W_P, mg
C10	0.0418	1.064	1.1704
C10=	0.3528	9.646	9.8784
C12	0	3.29	0
C12=	0	13.8264	0
C14	0	11.7908	0
C14=	0	149.1224	0
C16	2.4135	30.002	67.578
C16=	5.9701	229.922	167.1628
C20	3.5217	76.4148	98.6076
C22	2.5753	237.4288	72.1084
C24	3.7235	0	104.258
C28	3.9091	107.716	109.4548

Table A10: Concentration of components in the cracked product at 560˚C, 3minutes using synthesized zeolite Y

Component	C_P, mg/ml	W_{HGO}, mg	W_P, mg
C10	0.0345	1.14	1.035
C10=	0.3448	10.335	10.344
C12	0.0912	3.525	2.736
C12=	0.6657	14.814	19.971
C14	2.9745	12.633	89.235
C14=	3.0392	159.774	91.176
C16	4.6083	32.145	138.249
C16=	2.8145	246.345	84.435
C20	6.8122	81.873	204.366
C22	4.7939	254.388	143.817
C24	2.5031	0	75.093
C28	2.9172	115.41	87.516

Table A11: Concentration of components in the cracked product at 590˚C, 1minute using synthesized zeolite Y

C_{HGO}	Component	C_P, mg/ml	W_{HGO}, mg	W_P, mg
0.038	C10	0.0421	1.102	1.2209
0.3445	C10=	0	9.9905	0
0.1175	C12	0.2822	3.4075	8.1838
0.4938	C12=	0	14.3202	0
0.4211	C14	0	12.2119	0
5.3258	C14=	0	154.4482	0
1.0715	C16	5.0987	31.0735	147.8623
8.2115	C16=	2.7568	238.1335	79.9472
2.7291	C20	5.1087	79.1439	148.1523
8.4796	C22	9.0684	245.9084	262.9836
0	C24	0.9361	0	27.1469
3.847	C28	1.7632	111.563	51.1328

Table A12: ***Concentration of components in the cracked product at 590˚C, 2minutes using synthesized zeolite Y***

Component	C_P, mg/ml	W_{HGO}, mg	W_P, mg
C10	0.0341	1.178	1.0571
C10=	0	10.6795	0
C12	0.2355	3.6425	7.3005
C12=	0	15.3078	0
C14	0	13.0541	0
C14=	0	165.0998	0
C16	1.4803	33.2165	45.8893
C16=	7.0758	254.5565	219.3498
C20	10.1073	84.6021	313.3263
C22	5.9141	262.8676	183.3371
C24	1.2682	0	39.3142
C28	0.5347	119.257	16.5757

Table A13: ***Concentration of components in the cracked product at 590˚C, 3minutes using synthesized zeolite Y***

Component	C_P, mg/ml	W_{HGO}, mg	W_P, mg
C10	0.035	1.254	1.155
C10=	0.3432	11.3685	11.3256
C12	0.0963	3.8775	3.1779
C12=	0.5966	16.2954	19.6878
C14	0	13.8963	0
C14=	3.4774	175.7514	114.7542
C16	5.4911	35.3595	181.2063
C16=	1.1617	270.9795	38.3361
C20	6.4803	90.0603	213.8499
C22	4.9127	279.8268	162.1191
C24	2.7655	0	91.2615
C28	1.8329	126.951	60.4857

Calibration of standards on samples from commercial zeolite Y

Table A14: Concentration of components in the cracked product at 500˚C, 1minute using commercial zeolite Y

C_{HGO}	Component	C_P, mg/ml	W_{HGO}, mg	W_P, mg
0.038	C10	0.0505	0.456	0.606
0.3445	C10=	0.3657	4.134	4.3884
0.1175	C12	0.5826	1.41	6.9912
0.4938	C12=	1.0508	5.9256	12.6096
0.4211	C14	6.9291	5.0532	83.1492
5.3258	C14=	0.5531	63.9096	6.6372
1.0715	C16	2.3736	12.858	28.4832
8.2115	C16=	1.2074	98.538	14.4888
2.7291	C20	12.0248	32.7492	144.2976
8.4796	C22	5.8391	101.7552	70.0692
0	C24	1.2733	0	15.2796
3.847	C28	0.2634	46.164	3.1608

Table A15: Concentration of components in the cracked product at 500˚C, 2minutes using commercial zeolite Y

Component	C_P, mg/ml	W_{HGO}, mg	W_P, mg
C10	0.0361	0.57	0.5415
C10=	0.3467	5.1675	5.2005
C12	0.5693	1.7625	8.5395
C12=	0.6757	7.407	10.1355
C14	0.018	6.3165	0.27
C14=	1.3195	79.887	19.7925
C16	1.2312	16.0725	18.468
C16=	0.7146	123.1725	10.719
C20	3.8758	40.9365	58.137
C22	5.8735	127.194	88.1025
C24	4.5992	0	68.988
C28	2.9837	57.705	44.7555

Table A16: Concentration of components in the cracked product at 500°C, 3minutes using commercial zeolite Y

Component	C_P, mg/ml	W_{HGO}, mg	W_P, mg
C10	0.0335	0.646	0.5695
C10=	0.3428	5.8565	5.8276
C12	0.2252	1.9975	3.8284
C12=	0.4164	8.3946	7.0788
C14	0.018	7.1587	0.306
C14=	0.3431	90.5386	5.8327
C16	2.2704	18.2155	38.5968
C16=	0.2575	139.5955	4.3775
C20	10.3596	46.3947	176.1132
C22	4.4459	144.1532	75.5803
C24	0.8799	0	14.9583
C28	0.0292	65.399	0.4964

Table A17: Concentration of components in the cracked product at 530°C, 1minute using commercial zeolite Y

C_{HGO}	Component	C_P, mg/ml	W_{HGO}, mg	W_P, mg
0.038	C10	0.0388	0.57	0.582
0.3445	C10=	0.4255	5.1675	6.3825
0.1175	C12	0.4173	1.7625	6.2595
0.4938	C12=	0.4164	7.407	6.246
0.4211	C14	0.8618	6.3165	12.927
5.3258	C14=	0.4931	79.887	7.3965
1.0715	C16	4.8535	16.0725	72.8025
8.2115	C16=	3.2506	123.1725	48.759
2.7291	C20	8.6593	40.9365	129.8895
8.4796	C22	3.0273	127.194	45.4095
0	C24	2.6755	0	40.1325
3.847	C28	1.7084	57.705	25.626

Table A18: Concentration of components in the cracked product at 530˚C, 2minutes using commercial zeolite Y

Component	C_P, mg/ml	W_{HGO}, mg	W_P, mg
C10	0.0341	0.608	0.5456
C10=	0.3441	5.512	5.5056
C12	0.1656	1.88	2.6496
C12=	0.5084	7.9008	8.1344
C14	0.018	6.7376	0.288
C14=	0.3431	85.2128	5.4896
C16	0.0358	17.144	0.5728
C16=	5.3836	131.384	86.1376
C20	4.5715	43.6656	73.144
C22	3.5205	135.6736	56.328
C24	1.2042	0	19.2672
C28		61.552	0

Table A19: Concentration of components in the cracked product at 530˚C, 3minutes using commercial zeolite Y

Component	C_P, mg/ml	W_{HGO}, mg	W_P, mg
C10	0.8967	0.912	21.5208
C10=	1.8929	8.268	45.4296
C12	0.2863	2.82	6.8712
C12=	0.6952	11.8512	16.6848
C14	0.9127	10.1064	21.9048
C14=	0.6186	127.8192	14.8464
C16	0.3539	25.716	8.4936
C16=	0.5117	197.076	12.2808
C20	3.624	65.4984	86.976
C22	4.9265	203.5104	118.236
C24	2.7631	0	66.3144
C28	2.3053	92.328	55.3272

Table A20: ***Concentration of components in the cracked product at 560˚C, 1minute using commercial zeolite Y***

C_{HGO}	Component	C_P, mg/ml	W_{HGO}, mg	W_P, mg
0.038	C10	0.2165	0.608	3.464
0.3445	C10=	0.5025	5.512	8.04
0.1175	C12	1.2676	1.88	20.2816
	C12=	3.7851	0	60.5616
0.4211	C14	1.9018	6.7376	30.4288
5.3258	C14=	2.6031	85.2128	41.6496
1.0715	C16	0.0357	17.144	0.5712
8.2115	C16=	0.1575	131.384	2.52
2.7291	C20	6.5768	43.6656	105.2288
8.4796	C22	7.6372	135.6736	122.1952
0	C24	1.7129	0	27.4064
3.847	C28	2.7055	61.552	43.288

Table A21: ***Concentration of components in the cracked product at 560˚C, 2minutes using commercial zeolite Y***

Component	C_P, mg/ml	W_{HGO}, mg	W_P, mg
C10	0.116	0.646	1.972
C10=	0.4444	5.8565	7.5548
C12	0.8668	1.9975	14.7356
C12=	0.4164	0	7.0788
C14	1.7184	7.1587	29.2128
C14=	1.3431	90.5386	22.8327
C16	0.4657	18.2155	7.9169
C16=	2.0752	139.5955	35.2784
C20	5.0156	46.3947	85.2652
C22	3.6029	144.1532	61.2493
C24	1.0798	0	18.3566
C28	3.5203	65.399	59.8451

Table A22: ***Concentration of components in the cracked product at 560°C, 3minutes using commercial zeolite Y***

Component	C_P, mg/ml	W_{HGO}, mg	W_P, mg
C10	0.0346	0.988	0.8996
C10=	0.3444	8.957	8.9544
C12	0.1524	3.055	3.9624
C12=	0.5781	0	15.0306
C14	0.018	10.9486	0.468
C14=	0.3431	138.4708	8.9206
C16	6.1819	27.859	160.7294
C16=	3.5941	213.499	93.4466
C20	10.8791	70.9566	282.8566
C22	4.4076	220.4696	114.5976
C24	1.1263	0	29.2838
C28	0.1875	100.022	4.875

Table A23: ***Concentration of components in the cracked product at 590°C, 1minute using commercial zeolite Y***

C_{HGO}	Component	C_P, mg/ml	W_{HGO}, mg	W_P, mg
0.038	C10	0.0387	0.836	0.8514
0.3445	C10=	0.3473	7.579	7.6406
0.1175	C12	0.2773	2.585	6.1006
0.4938	C12=	0.7479	10.8636	16.4538
0.4211	C14	1.6718	9.2642	36.7796
5.3258	C14=	4.6897	117.1676	103.1734
1.0715	C16	3.3093	23.573	72.8046
8.2115	C16=	3.1568	180.653	69.4496
2.7291	C20	6.6278	60.0402	145.8116
8.4796	C22	5.7131	186.5512	125.6882
0	C24	2.2189	0	48.8158
3.847	C28	1.0409	84.634	22.8998

Table A24: Concentration of components in the cracked product at 590˚C, 2minutesusing commercial zeolite Y

Component	C_P, mg/ml	W_{HGO}, mg	W_P, mg
C10	0.0382	0.836	0.8404
C10=	0.3467	7.579	7.6274
C12	0.0292	2.585	0.6424
C12=	0.4164	10.8636	9.1608
C14	0.018	9.2642	0.396
C14=	0.3431	117.1676	7.5482
C16	3.1016	23.573	68.2352
C16=	2.6332	180.653	57.9304
C20	8.9179	60.0402	196.1938
C22	3.5009	186.5512	77.0198
C24	0.865	0	19.03
C28	0.1798	84.634	3.9556

Table A25: Concentration of components in the cracked product at 590˚C, 3minutesusing commercial zeolite Y

Component	C_P, mg/ml	W_{HGO}, mg	W_P, mg
C10	0.0406	1.026	1.0962
C10=	0.3481	9.3015	9.3987
C12	0.0292	3.1725	0.7884
C12=	0.4164	13.3326	11.2428
C14	0.318	11.3697	8.586
C14=	0.2431	143.7966	6.5637
C16	4.0689	28.9305	109.8603
C16=	3.6421	221.7105	98.3367
C20	1.3817	73.6857	37.3059
C22	6.6175	228.9492	178.6725
C24	1.1933	0	32.2191
C28	0.2332	103.869	6.2964

- Using zeolite Y/ZSM-5

Table A26: ***Concentration of components in the cracked product at 500°C, 1minute using Y/ZSM-5***

C_{HGO}	Component	C_P, mg/ml	W_{HGO}, mg	W_P, mg
0.0380	C10	0.0373	0.4940	0.4849
0.3445	C10=	0.3494	4.4785	4.5422
0.1175	C12	0.2831	1.5275	3.6803
0.4938	C12=	0.7763	6.4194	10.0919
0.4211	C14	0	5.4743	0
5.3258	C14=	0	69.2354	0
1.0715	C16	1.3118	13.9295	17.0534
8.2115	C16=	10.2721	106.7495	133.5373
2.7291	C20	7.7342	35.4783	100.5446
8.4796	C22	8.1867	110.2348	106.4271
0	C24	2.2994	0	29.8922
3.8470	C28	0.4078	50.0110	5.3014

Table A27: ***Concentration of components in the cracked product at 500°C, 2minutes using Y/ZSM-5***

Component	C_P, mg/ml	W_{HGO}, mg	W_P, mg
C10	0.0425	0.6080	0.6800
C10=	0.3579	5.5120	5.7264
C12	1.7798	1.8800	28.4768
C12=	1.1016	7.9008	17.6256
C14	0	6.7376	0
C14=	0	85.2128	0
C16	1.7541	17.1440	28.0656
C16=	3.5398	131.3840	56.6368
C20	9.2926	43.6656	148.6816
C22	3.6249	135.6736	57.9984
C24	1.1011	0	17.6176
C28	0.0163	61.5520	0.2608

Table A28: ***Concentration of components in the cracked product at 500˚C, 3minutes using Y/ZSM-5***

Component	C_P, mg/ml	W_{HGO}, mg	W_P, mg
C10	0.0490	0.6460	0.8330
C10=	0.3700	5.8565	6.2900
C12	1.5162	1.9975	25.7754
C12=	1.2492	8.3946	21.2364
C14	0	7.1587	0
C14=	0	90.5386	0
C16	2.3932	18.2155	40.6844
C16=	3.6659	139.5955	62.3203
C20	1.1392	46.3947	19.3664
C22	3.7460	144.1532	63.6820
C24	0.8125	0	13.8125
C28	0.1527	65.3990	2.5959

Table A29: ***Concentration of components in the cracked product at 530˚C, 1minute using Y/ZSM-5***

C_{HGO}	Component	C_P, mg/ml	W_{HGO}, mg	W_P,mg
0.0380	C10	0.7489	0.5700	11.2335
0.3445	C10=	0.6844	5.1675	10.2660
0.1175	C12	5.4942	1.7625	82.4130
0.4938	C12=	3.7632	7.4070	56.4480
0.4211	C14	0	6.3165	0
5.3258	C14=	6.0971	79.8870	91.4565
1.0715	C16	0	16.0725	0
8.2115	C16=	0	123.1725	0
2.7291	C20	2.6425	40.9365	39.6375
8.4796	C22	5.4583	127.1940	81.8745
0	C24	2.3179	0	34.7685
3.8470	C28	0.1426	57.7050	2.1390

Table A30: ***Concentration of components in the cracked product at 530˚C, 2minutes using Y/ZSM-5***

Component	C_P, mg/ml	W_{HGO}, mg	W_P,mg
C10	0.0845	0.6840	1.5210
C10=	0.4030	6.2010	7.2540
C12	0.7525	2.1150	13.5450
C12=	0.9763	8.8884	17.5734
C14	0	7.5798	0
C14=	0	95.8644	0
C16	8.2931	19.2870	149.2758
C16=	2.7565	147.8070	49.6170
C20	1.2115	49.1238	21.8070
C22	3.4998	152.6328	62.9964
C24	0.7747	0	13.9446
C28	0.1651	69.2460	2.9718

Table A31: ***Concentration of components in the cracked product at 530˚C, 3minutes using Y/ZSM-5***

Component	C_P, mg/ml	W_{HGO}, mg	W_P,mg
C10	0.5787	0.7220	10.9953
C10=	3.6578	6.5455	69.4982
C12	1.4330	2.2325	27.2270
C12=	6.0391	9.3822	114.7429
C14	3.9309	8.0009	74.6871
C14=	1.9545	101.1902	37.1355
C16	0	20.3585	0
C16=	0	156.0185	0
C20	0	51.8529	0
C22	0	161.1124	0
C24	2.1181	0	40.2439
C28	1.6635	73.0930	31.6065

Table A32: ***Concentration of components in the cracked product at 560˚C, 1minute using Y/ZSM-5***

C_{HGO}	Component	C_P, mg/ml	W_{HGO}, mg	W_P, mg
0.0380	C10	1.9001	1.1020	55.1029
0.3445	C10=	2.9676	9.9905	86.0604
0.1175	C12	2.1049	3.4075	61.0421
0.4938	C12=	4.4514	14.3202	129.0906
0.4211	C14	1.2612	12.2119	36.5748
5.3258	C14=	8.5295	154.4482	247.3555
1.0715	C16	2.1305	31.0735	61.7845
8.2115	C16=	3.7770	238.1335	109.5330
2.7291	C20	2.3269	79.1439	67.4801
8.4796	C22	8.6971	245.9084	252.2159
0	C24	2.2758	0	65.9982
3.8470	C28	0.6820	111.5630	19.7780

Table A33: ***Concentration of components in the cracked product at 560˚C, 2minutes using Y/ZSM-5***

Component	C_P, mg/ml	W_{HGO}, mg	W_P, mg
C10	0.3893	1.0640	10.9004
C10=	0.9734	9.6460	27.2552
C12	2.4901	3.2900	69.7228
C12=	3.5876	13.8264	100.4528
C14	1.3141	11.7908	36.7948
C14=	8.5721	149.1224	240.0188
C16	0	30.0020 229.9220	0
C16=	0	0	0
C20	2.8230	76.4148	79.044
C22	1.1899	237.4288	33.3172
C24	3.5191	0	98.5348
C28	1.1302	107.7160	31.6456

Table A34: Concentration of components in the cracked product at 560°C, 3minutes using Y/ZSM-5

Component	C_P, mg/ml	W_{HGO}, mg	W_P, mg
C10	0.0392	1.1400	1.1760
C10=	0.3497	10.3350	10.4910
C12	0.3781	3.5250	11.3430
C12=	0.7416	14.8140	22.2480
C14	0	12.6330	0
C14=	0	159.7740	0
C16	2.7075	32.1450	81.2250
C16=	7.2550	246.3450	217.6500
C20	7.8731	81.8730	236.1930
C22	7.6453	254.3880	229.3590
C24	1.9979	0	59.9370
C28	0.2295	115.4100	6.8850

Table A35: Concentration of components in the cracked product at 590°C, 1minute using Y/ZSM-5

C_{HGO}	Component	C_P, mg/ml	W_{HGO}, mg	W_P, mg
0.0380	C10	0.0761	1.0640	2.1308
0.3445	C10=	0.3885	9.6460	10.8780
0.1175	C12	2.2559	3.2900	63.1652
0.4938	C12=	1.3309	13.8264	37.2652
0.4211	C14	0	11.7908	0
5.3258	C14=	0	149.1224	0
1.0715	C16	8.1079	30.0020	227.0212
8.2115	C16=	2.7903	229.9220	78.1284
2.7291	C20	1.1653	76.4148	32.6284
8.4796	C22	4.5787	237.4288	128.2036
0	C24	1.0678	0	29.8984
3.8470	C28	0.1816	107.7160	5.0848

Table A36: Concentration of components in the cracked product at 590˚C, 2minutes using Y/ZSM-5

Component	C_P, mg/ml	W_{HGO}, mg	W_P, mg
C10	0.1601	1.1780	4.9631
C10=	0.6020	10.6795	18.6620
C12	3.5637	3.6425	110.4747
C12=	2.4089	15.3078	74.6759
C14	0	13.0541	0
C14=	0	165.0998	0
C16	0	33.2165	0
C16=	0	254.5565	0
C20	0	84.6021	0
C22	4.7380	262.8676	146.8780
C24	2.9319	0	90.8889
C28	0.2696	119.2570	8.3576

Table A37: Concentration of components in the cracked product at 590˚C, 3minutes using Y/ZSM-5

Component	C_P, mg/ml	W_{HGO}, mg	W_P, mg
C10	0.0587	1.292	1.9958
C10=	0.4441	11.713	15.0994
C12	1.1898	3.995	40.4532
C12=	0.9938	16.7892	33.7892
C14	0.9364	14.3174	31.8376
C14=	1.3556	181.0772	46.0904
C16	1.9094	36.431	64.9196
C16=	4.7787	279.191	162.4758
C20	1.5263	92.7894	51.8942
C22	9.2016	288.3064	312.8544
C24	1.7262	0	58.6908
C28	0.7588	130.798	25.7992

APPENDIX B: Material balance of heavy gas oil and its conversion

Appendix B shows the conversion of the heavy gas oil for the three catalysts used.

- Using synthesized zeolite Y

Table B1: ***Material balance of HGO used for cracking reaction at 500°C using synthesized zeolite Y***

volume of HGO, ml	volume of residual HGO, ml	time, min
40.0	31.0	0.5
40.0	27.0	1.0
40.0	25.0	2.0
40.0	22.0	3.0

Table B2: ***Material balance of HGO used for cracking reaction at 530°C using synthesized zeolite Y***

volume of HGO, ml	volume of residual HGO, ml	time, min
40.0	27.0	0.5
40.0	24.0	1.0
40.0	21.0	2.0
40.0	19.0	3.0

Table B3: ***Material balance of HGO used for cracking reaction at 560°C using synthesized zeolite Y***

volume of HGO, ml	volume of residual HGO, ml	time, min
40.0	16.0	0.5
40.0	15.0	1.0
40.0	12.0	2.0
40.0	10.0	3.0

Table B4: ***Material balance of HGO used for cracking reaction at 590°C using synthesized zeolite Y***

volume of HGO, ml	volume of residual HGO, ml	time, min
40.0	13.0	0.5
40.0	11.0	1.0
40.0	9.0	2.0
40.0	7.0	3.0

- Using commercial zeolite Y

Table B5: ***Material balance of HGO used for cracking reaction at 500°C using commercial zeolite Y***

volume of HGO, ml	volume of residual HGO, ml	time, min
40.0	31.0	0.5
40.0	28.0	1.0
40.0	25.0	2.0
40.0	23.0	3.0

Table B6: ***Material balance of HGO used for cracking reaction at 530°C using commercial zeolite Y***

volume of HGO, ml	volume of residual HGO, ml	time, min
40.0	30.0	0.5
40.0	25.0	1.0
40.0	24.0	2.0
40.0	16.0	3.0

Table B7: ***Material balance of HGO used for cracking reaction at 560°C using commercial zeolite Y***

volume of HGO, ml	volume of residual HGO, ml	time, min
40.0	28.0	0.5
40.0	24.0	1.0
40.0	23.0	2.0
40.0	14.0	3.0

Table B8: ***Material balance of HGO used for cracking reaction at 590°C using commercial zeolite Y***

volume of HGO, ml	volume of residual HGO, ml	time, min
40.0	25.0	0.5
40.0	18.0	1.0
40.0	18.0	2.0
40.0	13.0	3.0

➢ Using zeolite Y/ZSM-5

Table B9: ***Material balance of HGO used for cracking reaction at 500°Cusing zeolite Y/ZSM-5***

volume of HGO, ml	volume of residual HGO, ml	time, min
40.0	29.0	0.5
40.0	27.0	1.0
40.0	24.0	2.0
40.0	23.0	3.0

Table B10: ***Material balance of HGO used for cracking reaction at 530°C using zeolite Y/ZSM-5***

volume of HGO, ml	volume of residual HGO, ml	time, min
40.0	26.0	0.5
40.0	25.0	1.0
40.0	22.0	2.0
40.0	21.0	3.0

Table B11: ***Material balance of HGO used for cracking reaction at 560°C using zeolite Y/ZSM-5***

volume of HGO, ml	volume of residual HGO, ml	time, min
40.0	15.0	0.5
40.0	11.0	1.0
40.0	12.0	2.0
40.0	10.0	3.0

Table B12: ***Material balance of HGO used for cracking reaction at 590°C using zeolite Y/ZSM-5***

volume of HGO, ml	volume of residual HGO, ml	time, min
40.0	14.0	0.5
40.0	12.0	1.0
40.0	9.0	2.0
40.0	6.0	3.0

Conversion of the heavy gas oil using each catalyst was calculated using the formula and the result tabulated as shown in Tables B13 to B15 accordingly for each catalyst.

$$Conversion, X = \frac{volume\ of\ feed\ (HGO) - volume\ of\ residual\ feed}{volume\ of\ feed}$$

The volume of HGO and volume of residual feed can be obtained from Tables B1 to B12 to enable us calculate the conversion of HGO recorded in Tables B13 to B15 based on each catalysts used.

An example for the calculation of the conversion of HGO using synthesized zeolite Y at 0.5min and 500˚C from Table B1 can be shown below:

$$Conversion, X\ at\ 0.5min, 500^{\circ}\mathrm{C} = \frac{40 - 31}{40} = 0.225$$

Hence,

$Conversion, X\ at\ 0.5min, 500^{\circ}\mathrm{C} = 0.225$ shown in Table B13. This approach was also used to calculate the conversion at other conditions.

Table B13: Conversion of HGO using synthesized zeolite Y

time, sec	X_{500}	X_{530}	X_{560}	X_{590}
30	0.2250	0.3250	0.6000	0.6750
60	0.3250	0.4000	0.6250	0.7250
120	0.3750	0.4750	0.7000	0.7750
180	0.4500	0.5250	0.7500	0.8250

Table B14: Conversion of HGO using commercial zeolite Y

time, sec	X_{500}	X_{530}	X_{560}	X_{590}
30	0.2250	0.2500	0.3000	0.3750
60	0.3000	0.3750	0.4000	0.5500
120	0.3750	0.4000	0.4250	0.5500
180	0.4250	0.6000	0.6500	0.6750

Table B15: Conversion of HGO using zeolite Y/ZSM-5

time, sec	X_{500}	X_{530}	X_{560}	X_{590}
30	0.2750	0.3500	0.6250	0.6500
60	0.3250	0.3750	0.7250	0.7000
120	0.4000	0.4500	0.7000	0.7750
180	0.4250	0.4750	0.7500	0.8500

APPENDIX C: First order kinetic data for the synthesized zeolite Y

The following tables give the data for testing the order of the catalytic cracking reaction for the synthesized zeolite Y catalyst used.

Table C1: ***Conversion plot of data usingsynthesized zeolite Y at 500˚C for first order plot***

X_{500}	$1 - X_{500}$	$1/(1 - X_{500})$	Time, sec	$ln\left(1/(1 - X_{500})\right)$
0.2250	0.7750	1.2903	30	0.2548
0.3250	06750	1.4815	60	0.3930
0.3750	0.6250	1.6000	120	0.4700
0.4500	0.5500	1.8182	180	0.5978

Table C2: ***Conversion plot of data usingsynthesized zeolite Y at 530˚C for first order plot***

X_{530}	$1 - X_{530}$	$1/(1 - X_{530})$	Time, sec	$ln\left(1/(1 - X_{530})\right)$
0.3250	0.6750	1.4815	30	0.3930
0.4000	0.6000	1.6667	60	0.5108
0.4750	0.5250	1.9048	120	0.6443
0.5250	0.4750	2.1053	180	0.7444

Table C3: ***Conversion plot of data usingsynthesized zeolite Y at 560˚C for first order plot***

X_{560}	$1 - X_{560}$	$1/(1 - X_{560})$	Time, sec	$ln\left(1/(1 - X_{560}\right.$
0.6000	0.4000	2.5000	30	0.9162
0.6250	0.3750	2.6667	60	0.9808
0.7000	0.3000	3.3333	120	1.2039
0.7500	0.2500	4.0000	180	1.3862

Table C4: ***Conversion plot of data usingsynthesized zeolite Y at 590˚C for first order plot***

X_{590}	$1 - X_{590}$	$1/(1 - X_{590})$	Time, sec	$ln\left(1/(1 - X_{590})\right)$

0.6750	0.3250	3.0769	30	1.1239
0.7250	0.2750	3.6364	60	1.2909
0.7750	0.2250	4.4444	120	1.4916
0.8250	0.1750	5.7143	180	1.7429

APPENDIX D: Determination of order of reaction for commercial zeolite Y

The following tables give the data for testing the order of the catalytic cracking reaction for the commercial zeolite Y catalyst used.

- First order test

Table D1: ***Conversion plot of data using commercial zeolite Y at 500˚C for first order plot***

X_{500}	$1 - X_{500}$	$1/(1 - X_{500})$	Time, sec	$ln\left(1/(1 - X_{500})\right)$
0.2250	0.7750	1.2900	30	0.2546
0.3000	0.7000	1.4290	60	0.3569
0.3750	0.6250	1.6000	120	0.4700
0.4250	0.5750	1.7391	180	0.5533

Table D2: ***Conversion plot of data usingcommercial zeolite Y at 530˚C for first order plot***

X_{530}	$1 - X_{530}$	$1/(1 - X_{530})$	Time, sec	$ln\left(1/(1 - X_{530})\right)$
0.2250	0.7750	1.2900	30	0.2546
0.3000	0.7000	1.4290	60	0.3569
0.3750	0.6250	1.6000	120	0.4700
0.4250	0.5750	1.7391	180	0.5533

Table D3: ***Conversion plot of data usingcommercial zeolite Y at 560˚C for first order plot***

X_{560}	$1 - X_{560}$	$1/(1 - X_{560})$	Time, sec	$ln\left(1/(1 - X_{560})\right)$
0.3000	0.7000	1.4286	30	0.3566
0.4000	0.6000	1.6667	60	0.5108
0.4250	0.5750	1.7391	120	0.5533
0.6500	0.3500	2.8571	180	1.0498

Table D4: ***Conversion plot of data usingcommercial zeolite Y at 590˚C for first order plot***

X_{590}	$1 - X_{590}$	$1/(1 - X_{590})$	Time, sec	$ln\left(1/(1 - X_{590})\right)$
0.3750	0.6250	1.6000	30	0.4700
0.5500	0.4500	2.2222	60	0.7984
0.5500	0.4500	2.2222	120	0.7984
0.6750	0.3250	3.0769	180	1.1239

- Second order test

Table D5: ***Conversion plot of data usingcommercial zeolite Y at 500˚C for second order plot***

$time, sec$	$X_{500}/1 - X_{500}$	X_{500}	$1 - X_{500}$
30	0.2903	0.2250	0.7750
60	0.4285	0.3000	0.7000
120	0.6000	0.3750	0.6250
180	0.7391	0.4250	0.5750

Table D6: ***Conversion plot of data usingcommercial zeolite Y at 530˚C for second order plot***

$time, sec$	$X_{530}/1 - X_{530}$	X_{530}	$1 - X_{530}$
30	0.3333	0.2500	0.7500
60	0.6000	0.3750	0.6250
120	0.6666	0.4000	0.6000
180	1.5000	0.6000	0.4000

Table D7: ***Conversion plot of data usingcommercial zeolite Y at 560°C for second order plot***

$time, sec$	$X_{560}/1-X_{560}$	X_{560}	$1-X_{560}$
30	0.4285	0.3000	0.7000
60	0.6666	0.4000	0.6000
120	0.7391	0.4250	0.5750
180	1.8571	0.6500	0.3500

Table D8: ***Conversion plot of data usingcommercial zeolite Y at 590°C for second order plot***

$time, sec$	$X_{590}/1-X_{590}$	X_{590}	$1-X_{590}$
30	0.6000	0.3750	0.6250
60	1.2222	0.5500	0.4500
120	1.2222	0.5500	0.4500
180	2.0769	0.6750	0.3250

APPENDIX E: Determination of order of reaction for synthesized zeolite Y/ZSM-5

This appendix gives the data for plotting graphs for testing of order of reactions for synthesized zeolite Y/ZSM-5.

Table E1: Conversion plot of data usingzeolite Y/ZSM-5 at 500˚C for second order plot

$time, sec$	$X_{500}/1-X_{500}$	X_{500}	$1-X_{500}$	$1/1-X_{500}$
30	0.3793	0.2750	0.7250	1.3793
60	0.4814	0.3250	0.6750	1.4814
120	0.6667	0.4000	0.6000	1.6667
180	0.7391	0.4250	0.5750	1.7391

Table E2: Conversion plot of data usingzeolite Y/ZSM-5 at 530˚C for second order plot

$time, sec$	$X_{530}/1-X_{530}$	X_{530}	$1-X_{530}$	$1/1-X_{530}$
30	0.5384	0.3500	0.6500	1.5384
60	0.6000	0.3750	0.6250	1.6000
120	0.8181	0.4500	0.5500	1.8181
180	0.9047	0.4750	0.5250	1.9047

Table E3: Conversion plot of data usingzeolite Y/ZSM-5 at 560˚C for second order plot

$time, sec$	$X_{560}/1-X_{560}$	X_{560}	$1-X_{560}$	$1/1-X_{560}$
30	1.6667	0.6250	0.3750	2.6667
60	2.6363	0.7250	0.2750	3.6363
120	2.3333	0.7000	0.3000	3.3333
180	3.0000	0.7500	0.2500	4.0000

Table E4: Conversion plot of data usingzeolite Y/ZSM-5 at 590˚C for second order plot

$time, sec$	$X_{560}/1-X_{560}$	X_{560}	$1-X_{560}$	$1/1-X_{560}$
30	1.8571	0.6500	0.3500	2.8571
60	2.3333	0.7000	0.3000	3.3333
120	3.4444	0.7750	0.2250	4.4444
180	5.6667	0.8500	0.1500	6.6667

APPENDIX F: Experimental data for the Arrhenius plot

This appendix shows the data for testing the Arrhenius equation and also showing whether the experimental data are well correlated.

Table F1: Data for Arrhenius plot for synthesized zeolite Y

Temperature, ˚C	k_{synY}, s^{-1}	T, K	1/T, K^{-1}	$\ln k_{synY}$, s^{-1}
500	0.0021	773	0.0013	-6.1658
530	0.0023	803	0.0012	-6.0748
560	0.0032	833	0.0012	-5.7446
590	0.0040	863	0.0011	-5.5214

Table F2: Data for Arrhenius plot for commercial zeolite Y for first order kinetics

Temperature, ˚C	k_{comY1}, s^{-1}	T, K	1/T, K^{-1}	$\ln k_{comY1}$, s^{-1}
500	0.0019	773	0.0013	-6.2659
530	0.0038	803	0.0012	-5.5727
560	0.0042	833	0.0012	-5.4726
590	0.0037	863	0.0011	-5.5994

Table F3: Data for Arrhenius plot for commercial zeolite Y for second order kinetics

k_{comY2}	T, K	1/T, K^{-1}	$\ln k_{comY2}$
0.0029	773	0.0013	-5.8430
0.0071	803	0.0012	-4.9476
0.0087	833	0.0012	-4.7444
0.0085	863	0.0011	-4.7676

Table F4: Data for Arrhenius plot for zeolite Y/ZSM-5 for second order kinetics

T, K	$k_{Y/ZSM-5}$	1/T, K^{-1}	$\ln k_{Y/ZSM-5}$
773	0.0024	0.0013	-6.0322
803	0.0026	0.0012	-5.9522
833	0.0067	0.0012	-5.0056
863	0.0250	0.0011	-3.6888

APPENDIX G: Effect of time on conversion of HGO

This appendix shows the data for effect of time on conversion using synthesized and commercial zeolite Y and synthesized zeolite Y/ZSM-5.

Table G1: Effect of time on conversion of heavy gas oil using synthesized zeolite Y

time, sec	X_{500}	X_{530}	X_{560}	X_{590}
30	0.2250	0.3250	0.6000	0.6750
60	0.3250	0.4000	0.6250	0.7250
120	0.3750	0.4750	0.7000	0.7750
180	0.4500	0.5250	0.7500	0.8250

Table G2: Effect of time on conversion of heavy gas oil using commercial zeolite Y

Time, s	X_{500}	X_{530}	X_{560}	X_{590}
30	0.225	0.25	0.3	0.375
60	0.3	0.375	0.4	0.55
120	0.375	0.4	0.425	0.55
180	0.425	0.6	0.65	0.675

Table G3: Effect of time on conversion of heavy gas oil using zeolite Y/ZSM-5

Time, s	X_{500}	X_{530}	X_{560}	X_{590}
30	0.2750	0.3500	0.6250	0.6500
60	0.3250	0.3750	0.7250	0.7000
120	0.4000	0.4500	0.7000	0.7750
180	0.4250	0.4750	0.7500	0.8500

APPENDIX H: Effect of temperature on conversion of HGO

This appendix shows the data for effect of temperature on conversion using synthesized and commercial zeolite Y and synthesized zeolite Y/ZSM-5.

Table H1: ***Effect of temperature on conversion of heavy gas oil using synthesized zeolite Y***

Temperature	X_{30s}	X_{60s}	X_{120s}	X_{180s}
500	0.2250	0.3250	0.3750	0.4500
530	0.3250	0.4000	0.4750	0.5250
560	0.6000	0.6250	0.7000	0.7500
590	0.6750	0.7250	0.7750	0.8250

Table H2: ***Effect of temperature on conversion of heavy gas oil using commercial zeolite Y***

Temperature	X_{30s}	X_{60s}	X_{120s}	X_{180s}
500	0.2250	0.3000	0.3750	0.4250
530	0.2500	0.3750	0.4000	0.6000
560	0.3000	0.4000	0.4250	0.6500
590	0.3750	0.5500	0.5500	0.6750

Table H3: ***Effect of temperature on conversion of heavy gas oil using zeolite Y/ZSM-5***

T, ˚C	X_{30s}	X_{60s}	X_{120s}	X_{180s}
500	0.2750	0.3250	0.4000	0.4250
530	0.3500	0.3750	0.4500	0.4750
560	0.6250	0.7250	0.7000	0.7500
590	0.6500	0.7000	0.7750	0.8500

APPENDIX I: Determination of yield of middle distillates

This appendix shows the yield of kerosene and diesel fractions produced during the cracking reaction using the different catalysts.

The yield of each fraction is evaluated base on the equation

$$Yield, Y(wt\%) = \frac{weight\ of\ fraction,}{total\ weight\ of\ feed}$$

The weight of fractions (kerosene or diesel) and total weight of feed can be obtained at each condition from Tables A2 to A37 to enable us calculate the yield of the fractions, thus recorded in Tables I1 to I4 based on each catalysts used.

An example for the calculation of the yield of fractions using synthesized zeolite Y at 1 minute and 500˚C can be shown below:

Kerosene fractions include: C14, C14=, C16 and C16=

Diesel fractions include: C20, C22, C24 and C28

For example gasoline fraction,

Weight of fraction (kerosene) from synthesized zeolite Y at 500˚C and1min is obtained from Table A2.

$$weight\ of\ fraction = \sum W_p = C14 + C14_{=} + C16 + C16_{=}$$

$$weight\ of\ fraction = 57.9722 + 104.2288 + 22.3951 + 39.9989$$

$$weight\ of\ fraction = 224.5750mg$$

Total weight of feed (HGO) is obtained from Table A2

$$Total\ weight\ of\ feed = \sum W_{HGO} = C10 + C10 = + \cdots \dots \dots \dots \dots + C24 + C28$$

$$Total\ weight\ of\ feed = 0.4940 + 4.4785 + \cdots \dots \dots \dots \dots + 0 + 50.011 = 404.0322mg$$

Therefore, the yield of kerosene at 500˚C at contact time of 1minute is

$$Yield_{kerosene}(500\text{˚C}, 1\text{min}) = \frac{224.5750}{404.0322} \times 100 = 55.5834wt\%$$

This value is reflected in Table I1. This approach was also used to calculate the yield of kerosene and diesel fractions shown in Tables I1 to I4.

Table I1: Yield of kerosene fraction using synthesized zeolite Y

	T = 500˚C	T = 530˚C	T = 560˚C	T = 590˚C
$Y_{kerosene\ @1min}$	55.5834	57.5455	22.3067	25.2756
$Y_{kerosene\ @2min}$	46.9362	56.855	26.9748	27.5927
$Y_{kerosene\ @3min}$	37.4435	54.4953	43.2586	36.5927

Table I2: Yield of diesel fractionusing synthesized zeolite Y

	T = 500˚C	T = 530˚C	T = 560˚C	T = 590˚C
$Y_{diesel\ @1min}$	31.5209	39.0699	29.0932	54.004
$Y_{diesel\ @2min}$	29.6029	34.3073	44.0736	57.3508
$Y_{diesel\ @3min}$	20.7246	31.9034	54.7731	51.4315

Table I3: Yield of kerosene fraction using commercial zeolite Y

	T = 500˚C	T = 530˚C	T = 560˚C	T = 590˚C
$Y_{kerosene\ @1min}$	35.5163	30.4521	15.2357	41.34
$Y_{kerosene\ @2min}$	33.5121	18.6601	18.0961	19.61
$Y_{kerosene\ @3min}$	9.3068	7.6613	32.6235	26.6762

Table I4: Yield of diesel fraction using commercial zeolite Y

	T = 500˚C	T = 530˚C	T = 560˚C	T = 590˚C
$Y_{diesel\ @1min}$	62.4259	51.9003	60.0751	50.2356
$Y_{diesel\ @2min}$	55.8413	47.1122	42.4751	43.3416
$Y_{diesel\ @3min}$	50.5615	43.8214	53.4135	30.3035